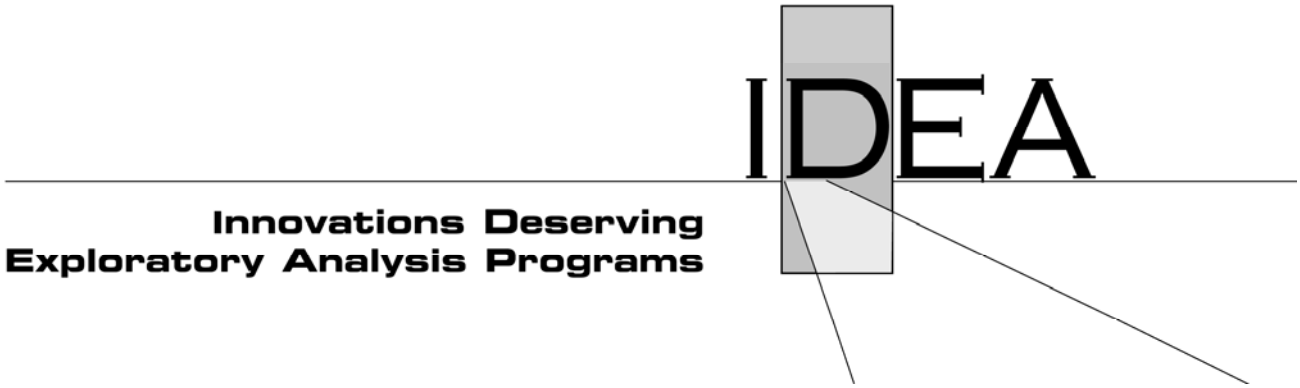


*High-Speed Rail Program*

# DEVELOPMENT OF A HYBRID UNI-AXIAL STRAIN TRANSDUCER FOR RAIL APPLICATIONS

Final Report for HRS-IDEA Project 15

Hosin "David" Lee, University of Utah, Salt Lake City, UT

*December 2001*

TRANSPORTATION RESEARCH BOARD □ NATIONAL RESEARCH COUNCIL

**INNOVATIONS DESERVING EXPLORATORY ANALYSIS (IDEA) PROGRAMS MANAGED BY THE TRANSPORTATION RESEARCH BOARD**

This investigation by University of Utah was performed as part of the High-Speed Rail IDEA program, which fosters innovative methods and technology in support of the Federal Railroad Administration's (FRA) next-generation high-speed rail technology development program.

The High-Speed Rail IDEA program is one of four IDEA programs managed by TRB. The other IDEA programs are listed below.

- NCHRP Highway IDEA, which focuses on advances in the design, construction, safety, and maintenance of highway systems, is part of the National Cooperative Highway Research Program.
- Transit IDEA focuses on development and testing of innovative concepts and methods for improving transit practice. The Transit IDEA Program is part of the Transit Cooperative Research Program, a cooperative effort of the Federal Transit Administration (FTA), the Transportation Research Board (TRB) and the Transit Development Corporation, a nonprofit educational and research organization of the American Public Transportation Association. The program is funded by the FTA and is managed by TRB.
- Safety IDEA focuses on innovative approaches to improving motor carrier, railroad, and highway safety. The program is supported by the Federal Motor Carrier Safety Administration and the Federal Highway Administration.

Management of the four IDEA programs is integrated to promote the development and testing of nontraditional and innovative concepts, methods, and technologies for surface transportation.

For information on the IDEA programs, contact the IDEA programs office by telephone (202-334-3310); by fax (202-334-3471); or on the Internet at http://www.nationalacademies.org/trb/idea

IDEA Programs
Transportation Research Board
500 Fifth Street, NW
Washington, DC 20001

## ACKNOWLEDGEMENTS

I gratefully acknowledges the financial support provided by the Transportation Research Borad's IDEA Program. Chuck Taylor of Transportation Research Board provided timely advice and guidance during several stages of this project. James Lungren of the Transportation Technology Center, Inc. acted as chairman of the project advisory committee and provided valuable technical information. I would like to acknowledge his assistance along with the contributions of other members of the project oversight committee: David Warnock and Crosby Mecham of Utah Transit Authority and Rick Campagna of Utah Department of Transportation.

Research assistance was provided by Hae-Bum Yun of the University of Utah and Mohammad Obadat of the University of Iowa. Brian Maclean and Robert Leatham of Sarcos, Inc. provided necessary technical information in conducting this research. Teresa Lopes of the Public Policy Center edited the report.

It has been a pleasure working with this great group of people from Utah, Colorado, Iowa and Washington, D.C.

**TABLE OF CONTENTS**

## LIST OF ACRONYMS

| | |
|---|---|
| LVDT | Linear Variable Differential Transformer |
| UAST | Uni-Axial Strain Transducer |
| RAM | Random Access Memory |
| IC | Integrated Circuit |
| MEMS | Micro-Electro-Mechanical System |
| VW | Vibrating Wire |
| LVDT | Linear Variable Differential Transformer |
| PIC | Programmable Integrated Circuit |
| TRB | Transportation Research Board |
| IDEA | Idea Deserving Exploratory Analysis |
| CMOS | Complementary Metal-Oxide Semiconductor |
| MTS | Mechanical Testing and Simulation |
| LED | Light Emitting Diode |
| PC | Personal Computer |

## LIST OF FIGURES

## LIST OF TABLES

## EXECUTIVE SUMMARY

It is extremely difficult to collect and analyse data on the fatigue history of high-speed railroad components such as rail, bridge members, and wheels using traditional data acquisition systems. Strain gauge systems typically require specialized signal processing devices, large power sources, and extensive wiring, which are generally not durable.

A Uni-Axial Strain Transducer (UAST) is a Micro-Electro Mechanical System (MEMS) with characteristics such as high resolution and high sampling rate, absolute encoding, no calibration requirements, no drift over time, and less measurement noise than analog-based strain sensors. As shown in Figure i, the UAST measures substrate strain by accurately measuring the displacement between two attachment pads. The distance between the pads is the gauge length for the device. When the substrate strains, displacement of one pad, relative to the pad on the other side of the package, causes the emitter, which is connected to the one pad through the moving flexture, to translate over the surface of the UAST IC chip. Strain is calculated by taking this measured transitional displacement and dividing it by the gauge length.

The UAST exploits the capacitive coupling between an array of electrostatic field emitters and an array of 64 field detectors on a UAST IC chip. The slightly different array element spacings form a vernier scale, and the system uses digital signal processing of the detector outputs to calculate the displacement of the emitter array relative to the detector array on a UAST IC chip. Displacements as low as 2.5 nm ($10^{-9}$ m) can be resolved. The sensor sampling rate is dynamically configurable and the sensor network can communicate with up to 128 UASTs on a common 5-wire digital bus, eliminating the need for shielding and considerably reducing the number of wires that must be routed through the structure to be measured. Because UASTs have low DC power requirements, they can be used in remote locations. The small size and on-chip signal processing features will make a UAST a truly portable testing device.

The research goal is to develop a prototype Hybrid Uni-Axial Strain Transducer (Hybrid UAST) that includes non-volatile RAM to store strain cycling history (e.g., tracking how many times the UAST crosses each of specified strain thresholds across its dynamic range), and to temporarily store the preprocessed data. The objective of this research is to determine the potential of the Hybrid UAST as a new tool to continuously monitor, analyze, and store the strain history of components such as rail. The resulting strain data can be periodically downloaded and used for such purposes as measuring rail stress induced by axle or thermal loadings. The prototype Hybrid UAST consists of three parts: a UAST sensor, a networking controller box, and a communication cable. A load cycle counting algorithm is integrated into a microcontroller, which is programmable using configuration switches.

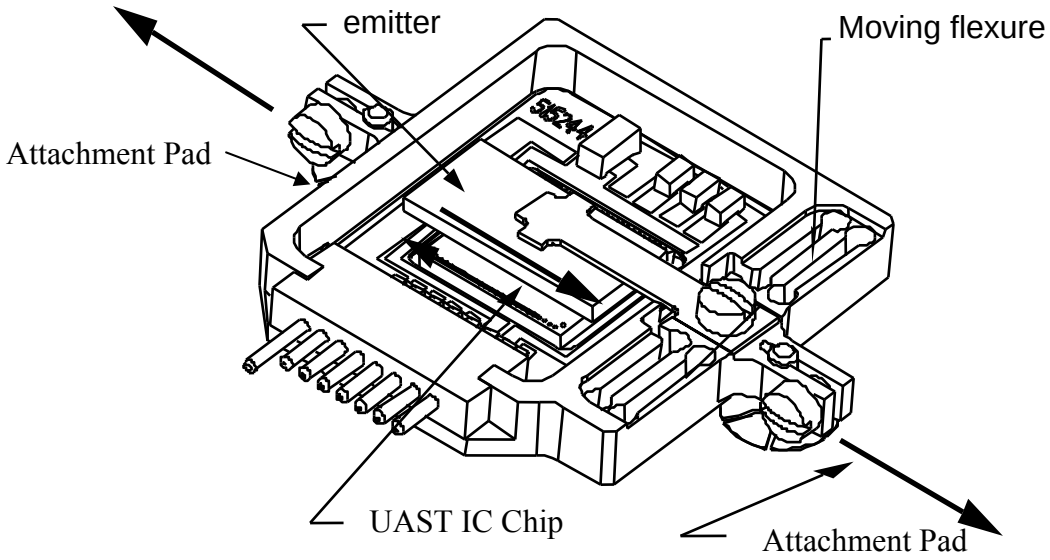


**FIGURE i. Schematic diagram of a UAST.**

Laboratory tests using an aluminum beam equipped with UASTs and conventional foil strain gauges demonstrated the accuracy and repeatability of the UASTs. For example, for the repeated measurements at a strain level of 95 με ($10^{-6}$), a standard deviation of 0.63 με was observed resulting in a very small coefficient of variation of 0.67%. In other words, approximately 95% of measurements were within 1.26 με. When the UAST data were compared against the mesaurements by foil strain gauges, there was an approximately 3% discrepancy between two sets of measurements. A series of cyclic loading tests was then performed to simulate a moving trainload applied on a rail using an MTS fatigue loading machine in the laboratory. Overall, these laboratory test results indicate that the UAST is accurate and repeatable in a wide range of strain values from 0 to 2,000με. An ideal technique for mounting the UAST on a rail was also developed by creating separate detachable mounting pads for the UAST. A project panel meeting was held to review the project objectives and approach. The panel indicated that the proposed Hybrid UAST could be suitable for monitoring track and bridge structures at remote locations, and for estimating their remaining service life in the interest of maintenance planning. The panel proposed additional potential application areas, including a train presence detection device, wireless instrumented wheel sets, a portable weigh-in-motion device, and a device to predict buckling of the rail.

A prototype Hybrid UAST package suitable for field application has been fabricated. In addition, two computer programs were developed for data acquisition and data analysis. The data acquisition program was used to operate the Hybrid UAST from a laptop computer, and the data analysis program was used to implement the peak searching and cycle counting algorithms. Raw data were collected to verify the cycle counting algorithm implemented in the Hybrid UAST in an outdoor operating environment. A prototype Hybrid UAST design and load cycle counting algorithm has been tested using actual strain data taken from a rail at the field test sites in Salt Lake City and Iowa City. Figure ii shows the controller and the UAST installed on the rail for real-time data acquisition. The raw data collected at 290 Hz (14-bit mode of UAST) without a train consistently showed a standard deviation of around 1.25 με. In other words, approximately 99.7% of background noises are less than 3.75 με. This level of error can be considered small relative to a peak strain range of 400 με caused by a typical trainload. The raw data collected at the same frequency with a train were also processed by the Hybrid UAST to accurately determine not only the number of load cycles but also the magnitudes of the peak loads, which are consistent with both laboratory measurements and theoretical calculations. In conclusion, both laboratory and field testing of the prototype Hybrid UAST with respect to its repeatability, accuracy, and viability in hybridization can be considered a great success. The positive results from this study warrant a continued research effort to develop a more refined commercial-grade Hybrid UAST that is sufficiently rugged to withstand harsh railroad operating environments.

**FIGURE ii. Strain data collection from a rail using UAST™ and a microcontroller.**

## IDEA PRODUCT: HYBRID UNI-AXIAL STRAIN TRANSDUCER

The project of evaluating the Uni-axial Strain Transducer (UAST) for potential application in high-speed railroad structures was initiated on November 16, 1998. The initial duration of the test was 1 year, and it was later extended by 4.5 months, to March 31, 2000. The UAST is theoretically a digital extensometer, not a strain gauge, which was originally developed for fatigue analysis of airplane frames (Maclean 1997). The main objective of this research project is to develop a Hybrid UAST that incorporates strain data reduction algorithms for railroad application (Yun 1999).

Most real-time strain monitoring systems collect enormous amounts of data, only a small fraction of which is useful. The prototype Hybrid UAST, however, will require only periodic downloading of fatigue data from the rail infrastructure. Consequently, the impact of a Hybrid UAST on the railroad industry will be significant because the commercialized version of this device can provide an instant computation of remaining service life for a rail infrastructure at a fraction of the cost of other real-time monitoring systems. The performance of the commercial-grade Hybrid UAST should compare favorably in both price and performance with other real-time sensors. Eventually, the proposed commercial-grade sensor will revolutionize the way strain data are collected and processed in practice.

The proposed commercial-grade Hybrid UAST will have a significant impact on the following transportation practices:

- monitoring railroad and bridge structures at remote locations,
- estimating the remaining service life of structures for maintenance planning,
- developing grade crossing warning devices (-using the UAST's ability as a presence detector),
- developing 2$^{nd}$ generation wheel set and freight car designs,
- developing portable weigh-in-motion devices,
- predicting buckling of the rail due to excessive thermal expansion, and
- continuously monitoring high-speed rail systems.

## CONCEPT AND INNOVATION

There are an increasing number of sensors, originally developed for aerospace industry, being modified for its immediate application in transportation infrastructure today. However, the application of such sensors has been slow because the materials used in transportation infrastructure are not as uniform or consistent as the materials used for aerospace frames. The objective of the proposed research is to determine a potential of the Hybrid Uni-Axial Strain Transducer (UAST) as a new tool to periodically, i.e., only once a month, monitor the structural capacity of the transportation infrastructure at a lower cost.

We developed a prototype Hybrid UAST which includes non-volatile RAM to store the strain cycling history of the UAST device, e.g., tracking how many times the UAST crosses each of ten strain thresholds across its dynamic range, and temporarily storing the preprocessed data. The prototype Hybrid UAST was successfully developed as a logical extension of UAST to allow the UAST to periodically download fatigue-related strain data from a rail. It could be used to provide meaningful predictions of remaining fatigue life for the rail infrastructure to which the Hybrid UAST is installed.

Both laboratory and field evaluations of the UAST were conducted to determine the accuracy of the UAST and a potential capability of preprocessing data, i.e., capturing the data exceeding a certain threshold level and temporarily storing the preprocessed data. To determine the accuracy of UAST, Strains measured by UASTs were compared with those measured by electrical resistance strain gauges. Cyclic loading tests were conducted to simulate the moving trainloads on a rail to determine optimum sampling rates and resolutions at various train speeds. In order to develop a prototype Hybrid UAST, a data acquisition program to operate the Hybrid UAST in the field was developed. Next, a peak searching algorithm and a cumulative cycle counting procedure were developed and programmed in the software package. The peak searching and cumulative cycle counting procedures were then integrated into CMOS IC chip of prototype Hybrid UAST to process strain data for estimating fatigue life of a rail. In addition, an optimum installation technique was developed to make the UAST a truly portable device. A "bonding jig" was developed to mount pads on a rail surface. Consequently, the UAST can be plugged into the mounting pads and be easily removed for a later use.

Laboratory tests using an aluminum beam equipped with UASTs and conventional foil strain gauges demonstrated the accuracy and repeatability of the UASTs. For the repeated measurements, at the mean value of 94.75 με, a very small standard deviation such as 0.63 με was obtained (see table 3). This represents that 95% of the measurements are within 93.49 and 96.01 με. When the UAST data were compared against the mesaurements by foil strain gauges, they were lower than the ones measured by foil strain gauges by 5.35 με (see table 3). Overall, there was an average 3% discrepancy between two sets of measurements (see figure 7). These laboratory test results indicate that the UAST is accurate and repeatable in a wide range of strain values from 0 to 2,000με (see figure 7). The raw data collected by the UAST without a trainload repeatedly showed also a very small standard deviation of 1.25 με (see figure 12), but twice as much as the ones measured in the laboratory. This level of error can be considered small enough to accurately measure a peak strain level up to 400 με caused by a typical trainload. The raw data collected with a train were also processed by the Hybrid UAST to accurately determine not only the number of load cycles but also magnitudes of the peak loads that were consistent with the laboratory and field data. Based on the accurate and repeatable test results obtained from both laboratory and field, it can be concluded that the Hybrid UAST is suitable for rail infrastructure applications.

The research efforts described in this report demonstrates an exploitation of a new class of strain sensors and sensor network architecture and a development of a prototype hybrid sensor which possesses: 1) digital, absolute encoding of strain with no drift over time, 2) minimum number of wires with no required shielding, 3) multiple strain sensors on a common bus, 4) variable sample rate and device resolution with synchronous event sampling, 5) low actuation force providing simple and reliable bonding to surfaces, 6) low cost, mass producibility using standard CMOS technology, 7) specially designed “smart” sensor for rail infrastructure, and 8) on-chip data preprocessing and storage capability.

# LITERATURE REVIEW

Railroad track consists of rails, ties, fastening components, ballast bed and subgrade. Steel rail, the most visible component of rail track, fulfills two major functions—it supports vehicles and guides them via the wheel flange on the interior side of the wheels. The wear on the head and gage face of rail is one of main determinants of service life. Fatigue defects are not normally a major concern for high speed, light axle load passenger operations using modern rail steels but they have become the significant factor in determining rail life in many heavy rail traffic corridors. One of the most difficult aspects of fatigue life estimation is obtaining accurate strain history data. In the area of strain measurement, there are many types of sensors currently on the market (see Table 1). Each sensor has different characteristics, and the selection of a sensor should depend on its application and purpose. For example, a traditional electric resistance strain gauge is the most widely used strain transducer for various applications. However, such gauges appear to be inadequate in fatigue measurement, especially in long-term field testing, because of their relatively high non-linearity, drifting over time, self-heat effect, and weakness against harsh environments (Neubert 1975). The operational principles and characteristics of each sensor are summarized below.

## ELECTRICAL RESISTANCE STRAIN GAUGES

The electrical resistance strain gauge is one of the most accurate, versatile and important types of sensors in stress analysis and measurement. During the past fifty years, it has been considered the standard strain-measuring device due to its relatively low cost and the variety of sizes and materials it comes in. There are two main types of such strain gauges: the wire strain gauge and the foil strain gauge.

Various types of material have been used in making strain gauges to achieve the following desirable features: 1) low and controllable temperature coefficient of resistance for good temperature compensation, 2) wide operating temperature range for the widest range of applications, 3) linear strain sensitivity in elastic range, 4) high resistivity for smallest size, 5) low hysteresis for repeatability and accuracy, 6) high strain sensitivity for maximum electrical output for given strain, and 7) good fatigue life for dynamic measurements (Charlmers 1982). For example, to minimize temperature sensitivity, a strain gauge can be made of copper-nickel alloy, which has a low temperature coefficient of resistance ($2\times10^{-5}$/°C). Normally, the fatigue limit for foil strain gauges is defined as the point at which the zero shift has a value of between 100 and 300 microstrain. The lengths of gauge range from 0.008 in (0.20 mm) to 4.00 in (102 mm) with a thickness ranging from 0.003 to 0.005 mm. The “piezo resistivity,” which represents strain-induced changes in resistivity (piezoresistive effect), is small (around 0.4) leading to a small gauge factor of around 2.0. A typical resistance strain gauge has the following specification (Simpson 1996):

- a gauge factor of 2.0 to 2.2;
- an unstrained resistance of 120 and 350 ohms;
- maximum tensile strain of $+2\times10^{-2}$ ε;
- maximum compressive strain of $-1\times10^{-2}$ ε;
- maximum operating temperature of 150°C;
- elongation capacity up to 5% of gauge length.

## SEMICONDUCTOR STRAIN GAUGE

In the 1950s, a number of U.S. laboratories conducted experiments on the piezo resistance effect in semiconductors and discovered that the piezoelectric effect of semiconductors could be much greater than that of conductors (Gandhi 1992). In semiconductor strain gauges, the "piezo resistive" term is large, leading to a large gauge factor(50 to 200). For example, a typical semiconductor sensitivity is 1000 V/ε, while that of a foil strain gauge (conductor) is 30 V/ε (Baker 1982).

**Table 1. Comparisons of Various Strain Transducers**

| Type | Foil | Semiconductor | LVDT | Vibrating Wire | PZT Film | PZT Ceramic | Optical Fiber | UAST (MEMS) |
|---|---|---|---|---|---|---|---|---|
| Typical Sensitivity | 30 V/ε | 1,000 V/ε | – | – | 10,000 V/ε | 20,000 V/ε | – | – |
| Bandwidth | 10 kHz | 100 kHz | 100 Hz | 100 Hz | 100 MHz | 100 MHz | 100 MHz | 2350 Hz |
| Maximum Strain Range | | | | ±2,000 με | | | | ±5,760 με |
| Gauge Lengths | 0.5 mm ~ 100 mm | 1 mm | 0.5 mm ~ 600mm | mm ~ cm | mm ~ m | mm ~ cm | mm ~ m | 10 mm |
| Point or Integrated | point | Point | point | point | integrated | point | integrated | point / integrated |
| Distributed Measurement Potential | no | no | no | no | yes | no | yes | no |
| Multiplexing Feasibility | difficult (field bus) | difficult (field bus) | difficult (field bus) | difficult (field bus) | possible | difficult (field bus) | good | excellent (up to 128) |
| Chemical Resistance | poor | good | poor | good | poor | pool | excellent | good |

## LINEAR VARIABLE DIFFERENTIAL TRANSFORMER

The measurement principle of the Linear Variable Differential Transformer (LVDT) is based on the theory of magnetics which states that a small fraction of movement can be detected by suitable signal conditioning electronics. The LVDT's high accuracy and repeatability enabled it to become one of the most popular displacement measurement methods. One of its main advantages is that there is no physical contact across the sensing element, which makes it suitable for the most arduous applications. The elongation limit of LVDT ranges from ±0.25mm to ±25cm.

## VIBRATING WIRE STRAIN GAUGE

The vibration wire (VW) strain gauge consists of a thin steel wire tensioned by two anchorages, and an electromagnetic coil, which detects the displacement of the steel wire by a change in voltage. When the distance between the two anchorages changes, the tension and natural frequency of wire is changed. Strain is proportional to the square of the length, and mass per unit length is inversely proportional to Young's modulus. Since the VW gauge can provide stable measurement values over a long period of time, it is applicable in measuring the long-term performance of a variety of materials, including concrete. The precision of the VW gauge is 10 με, with a measurement range of ±2,000με at the data collection frequency of 1,100 Hz.

## PIEZOELECTRIC STRAIN GAUGE

Piezoelectricity is defined as "an electric polarization produced by mechanical strain in crystals, where the polarization is assumed to be proportional to the strain and changes signs with the strain. Generally, piezoelectric materials used in instrument transducers can be classified into two groups. The first includes natural piezoelectric crystals such as quartz, and the second covers polarized piezoelectric ceramics such as barium titanate. If a thin piezoelectric material is cemented to a structure under stress, the stress causes strain in the structure and the piezoelectric material. The stress is then transmitted to the piezoelectric material, and a charge is generated across the crystal.

## MICRO-ELECTRO-MECHANICAL SYSTEM

Integrated micro-electro-mechanical systems (MEMS) can be defined as "monolithic chips that combine micro-mechanical elements and electronic circuitry." The co-fabrication of micro-mechanical devices and integrated circuits has advantages in signal conditioning and processing. Due to the small size of micro-mechanical devices, their output signals are extremely small in magnitude. Without on-chip signal conditioning circuitry, these weak signals can be overwhelmed by noise or disturbance. On-chip conditioning circuitry can also compensate for temperature drift or other nonlinearities in sensor characteristics.

The hybrid method, where different chips—including electronics, sensors and actuators—are placed in a single package and connected by wire bonding, has long been adopted as the industry standard. This approach is very flexible, and there are few restrictions on the types of useable electronics and substrates. However, hybrids cannot be batch-fabricated, and could suffer from system performance degradation due to stray or large capacitance.

The monolithic integration of MEMS sensors and actuators can be performed within the same substrate as the electronics. This embedded method is suitable for batch processing, and results in a significantly improved performance. However, it involves a fairly large number of processing steps, resulting in increased processing complexity and reduced yield, and thus increasing the cost of production. The direct flip chip method of attaching MEMS and electronics has been demonstrated as a viable manufacturable alternative in smart MEMS development. In the flip chip method, the electronics and the MEMS are fabricated on different substrates, and are directly connected using solder bumps.

## UNI-AXIAL STRAIN TRANSDUCER

Figure 1 is a schematic diagram of a Uni-Axial Strain Transducer (UAST), which is a kind of MEMS. Figure 2 demonstrates how the UAST measures substrate strain by accurately measuring the displacement between two attachment

pads in the opposite directions of the arrows. The distance between the pads is the gauge length for the device. When the substrate strains, displacement of one pad, relative to the pad on the other side of the package, causes the emitter, which is connected to the one pad through the moving flexure, to translate over the surface of the UAST IC chip. Strain is calculated by taking this measured transitional displacement and dividing it by the gauge length. The UAST exploits the capacitive coupling between an array of electrostatic field emitters and an array of 64 field detectors on a UAST IC chip. The slightly different array element spacings form a vernier scale, and the digital signal processing of the detector outputs is used to calculate the absolute translational displacement of the emitter array relative to the detector array in the UAST IC chip. The UAST provides a dynamic range of 11,500 με and displacements as low as 2.5 nm can be resolved. The sensor sampling rate is dynamically configurable for 150, 290, 540, 1000, 1600, or 2500 HZ, providing 15, 14, 13, 12, 11, or 10 bits of resolution (equal to 0.35, 0.7, 1.4, 2.8, 5.6, 11.4 με), respectively. The sensor network can communicate with up to 128 UASTs on a common 5-wire digital bus, eliminating the need for shielding and considerably reducing the number of wires that have to be routed through the structure being measured.

This new class of strain sensor and sensor network architecture possesses a number of important and unique features, including 1) digital, absolute encoding of strain with no drift over time, 2) minimum numbers of wires that do not require shielding, 3) multiple sensor types (strain, acceleration, temperature, etc) on a common network bus, 4) variable sample rate and device resolution with synchronous event sampling, 5) low actuation force providing simple and reliable bonding to surfaces, and 6) low cost and mass producibility using standard CMOS technology.

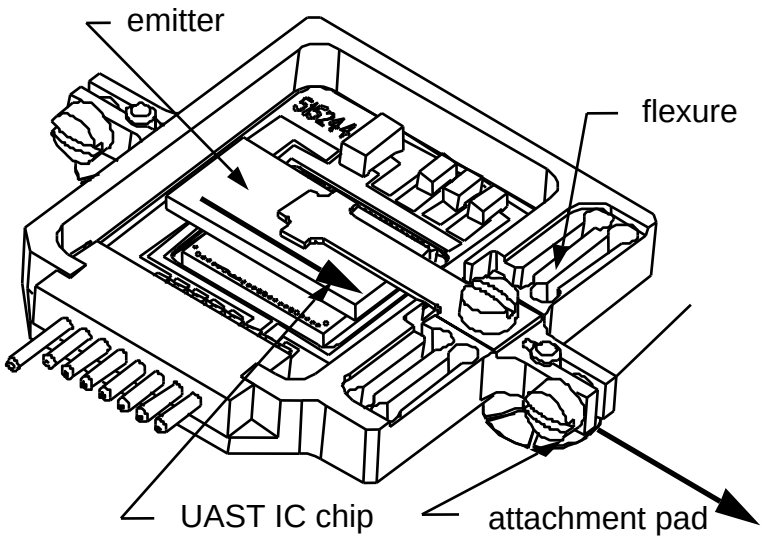


**Figure 1. Schematic of Uni-Axial Strain Transducer (UAST).**

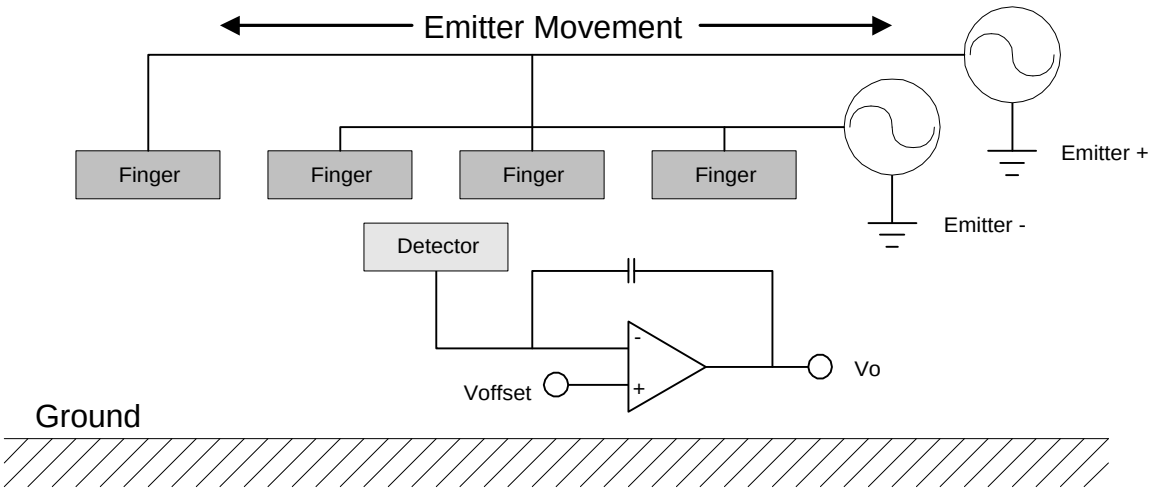


**Figure 2. Emitter fingers and detector of UAST.**

## LABORATORY TESTING OF THE UAST

Both cyclic tensile and static bending tests were performed on an aluminum beam instrumented with UASTs and electrical resistance strain gauges at the laboratory. The static bending test was also performed on a concrete beam instrumented with UASTs and electrical resistance strain gauges. Electrical resistance foil strain gauges were mounted next to the UAST to determine the accuracy of the device. Strain data were collected simultaneously from UASTs and electrical resistance strain gauges while the specimens were gradually loaded.

First, four-point bending tests were performed on a standard 6511 aluminum alloy beam of known properties (see Table 2) instrumented with UASTs and electrical resistance strain gauges. Figure 3 shows how the traditional resistance strain gauges were mounted next to the UAST to evaluate its accuracy. Strain data were collected from two UASTs—one mounted on top and one on the bottom of the test beam—using the UAST network controller as the specimens were being statically loaded. A series of cyclic loading tests was also performed on the same standard aluminum beam instrumented with the UASTs. Again, strain data were collected from two UASTs using the UAST network controller as the specimens were being loaded. The strain values measured by the UAST at various sampling rates were evaluated against the calculated strain values under known cyclic loads at the laboratory.

**Table 2. Mechanical Properties of 6511 Aluminum Alloy**

| | |
|---|---|
| Specification | QQ-A-200/8 |
| Form | Extruded rod, bar, and shapes |
| Condition | Aluminum-T6511 |
| Cross-sectional area | $\leq 32$ in$^2$ |
| Thickness or diameter | $\leq 1.000$ in |
| Elastic Modulus (Tension), | 9.9 ksi |
| Elastic Modulus (Compression) | 10.1 ksi |
| Shear Modulus | 3.8 ksi |
| Poisson's ratio | 0.33 |

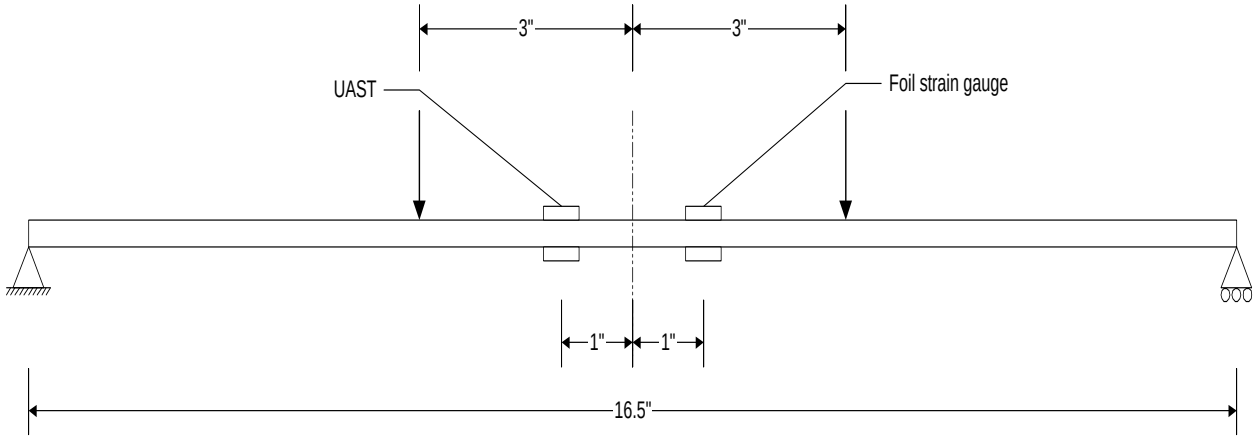


**Figure 3. Schematic diagram of bending beam experiment setup**

## STATIC BENDING TEST OF ALUMINUM BEAM INSTRUMENTED WITH UAST

Two UASTs and foil strain gauges were mounted on the top and bottom of the aluminum alloy beam. The gauges on top measure compressive strains while those on the bottom measure bending strains. Strains were measured from 0 to 100με at 10με increments, from 100 to 1,000με at 100με increments, and from 1,000 to 2,000με at 250με increments. For each given strain level, 20 readings were obtained using a UAST. The mean values and their standard deviations were computed for each strain level, and measurements were compared against the strain values measured by foil strain gauges mounted at the same location. As an example, the 20 UAST strain measurements taken at the 100με compressive strain level are summarized in Table 3, along with their mean (94.75 με) and standard devation (0.63 με) The percent error of the UAST (5.25% for the example in Table 3) was computed by dividing their mean value by the measurement obtained by the foil strain gauge.

A small discrepancy was observed between the measurements by the UAST and the foil resistance strain gauge, as is indicated in Figure 4. The percent errors were plotted against the strain levels as shown in Figure 5. Average errors for two sets of measurement were 3.98% (UAST1) and 3.08% (UAST2), respectively. An average 3 or 4 percent error should be considered quite reasonable given that UAST and foil strain gauges may not have been installed at the exactly same distances from the point of loading. In addition, these errors could have been also caused by a 0.045 inch gap between the specimen surface and the emitter/beam of the UAST, which would have over-estimated the tensile strains at the bottom of the beam while under-estimating compressive strains at the top of the beam. This type of discrepancy, which was caused by a known UAST design parameter, can be easily calibrated. Overall, these laboratory test results seem to indicate that the UAST is accurate and repeatable in a wide range of strain values from 0 to 2,000με.

## CYCLIC TENSILE TEST OF ALUMINUM BEAM INSTRUMENTED WITH UAST

A series of cyclic loading tests was performed to simulate a moving trainload applied on a rail using an MTS fatigue loading machine at the laboratory as shown in Figure 6. Cyclic strain data were collected using the UAST at various data collection frequencies and resolutions. The main goal of this experiment was to determine an optimum sampling rate to provide maximum resolution at the rate needed for a rail application.

A load-controlled cyclic loading test was performed with a given sinusoidal load. The sinusoidal load frequency was fixed at 9 Hz, which represented a moving wheel load at 15 mph. Strain data were collected at four different modes of UAST setting—12 bit, 13 bit, 14 bit and 15 bits—to provide different sampling rates and resolutions. Five thousand samples of longitudinal and transverse strains were collected for each operational mode at 12 bit, 13 bit, 14 bit and 15 bit. The maximum amplitude of transverse strain was approximately 30 percent that of longitudinal strain, which is quite close to a known Poisson's ratio of the aluminum alloy ($\nu = 0.33$).

Averages and standard deviations of peak and valley strain measurements for 12, 13, 14 and 15 bit modes are summarized in Tables 4 and 5. The results show that the averages peak strains were measured at 653.54, 640.64, 629.47, 622.82 and 636.62 με, and that those of valley strains were at 91.03, 97.64, 110.65 and 132.65 με for 12 bit, 13 bit, 14 bit and 15 bit modes, respectively. The number of data points collected at each loading cycle are summarized in Table 6 for each mode of operation. To estimate the number of data points collected at the higher train speed of 120 mph, the number of data points collected at 8 Hz (15 mph) was simply extrapolated up to 64 Hz as shown in the table. Assuming that at least 10 data points per cycle are needed to avoid "aliasing" errors, 12 bit mode or higher is recommended for collecting strain data from the rail subjected to a moving train at 120 mph.

**Table 3. Strain Measurements by Foil Strain Gauge and UAST (100με strain level)**

| Foil | UAST | | |
|---|---|---|---|
| Strain (με) | Strain (με) | Average (με) | Standard Deviation |
| 100 | 94.92 | 94.75 | 0.63 |
| | 94.92 | | |
| | 94.92 | | |
| | 94.23 | | |
| | 96.29 | | |
| | 93.54 | | |
| | 95.60 | | |
| | 94.92 | | |
| | 94.23 | | |
| | 94.23 | | |
| | 94.23 | | |
| | 94.23 | | |
| | 94.92 | | |
| | 94.23 | | |
| | 94.92 | | |
| | 94.92 | | |
| | 94.92 | | |
| | 95.60 | | |
| | 94.23 | | |
| | 94.92 | | |

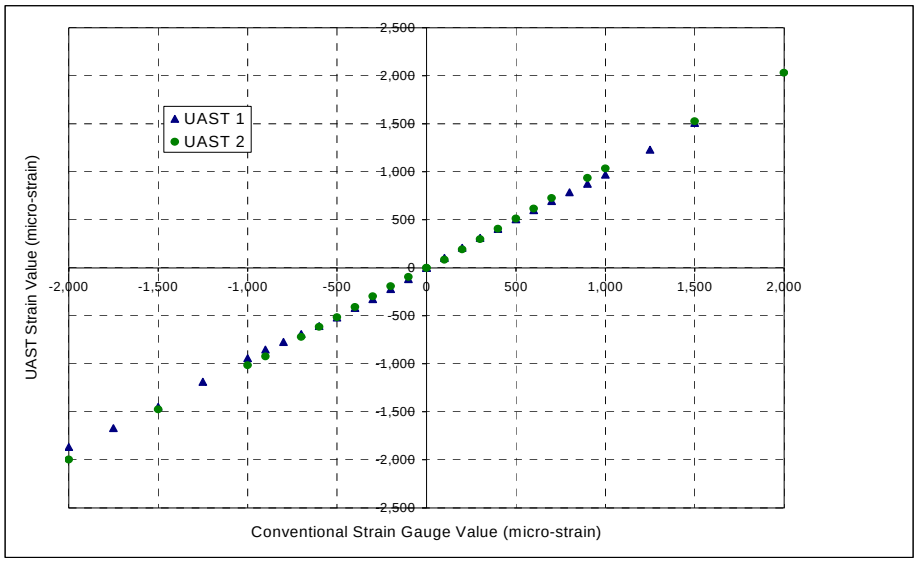


**Figure 4. Comparison of Two Sets of Strain Measurements by Foil Strain Gauge and UAST (UAST 1 and 2).**

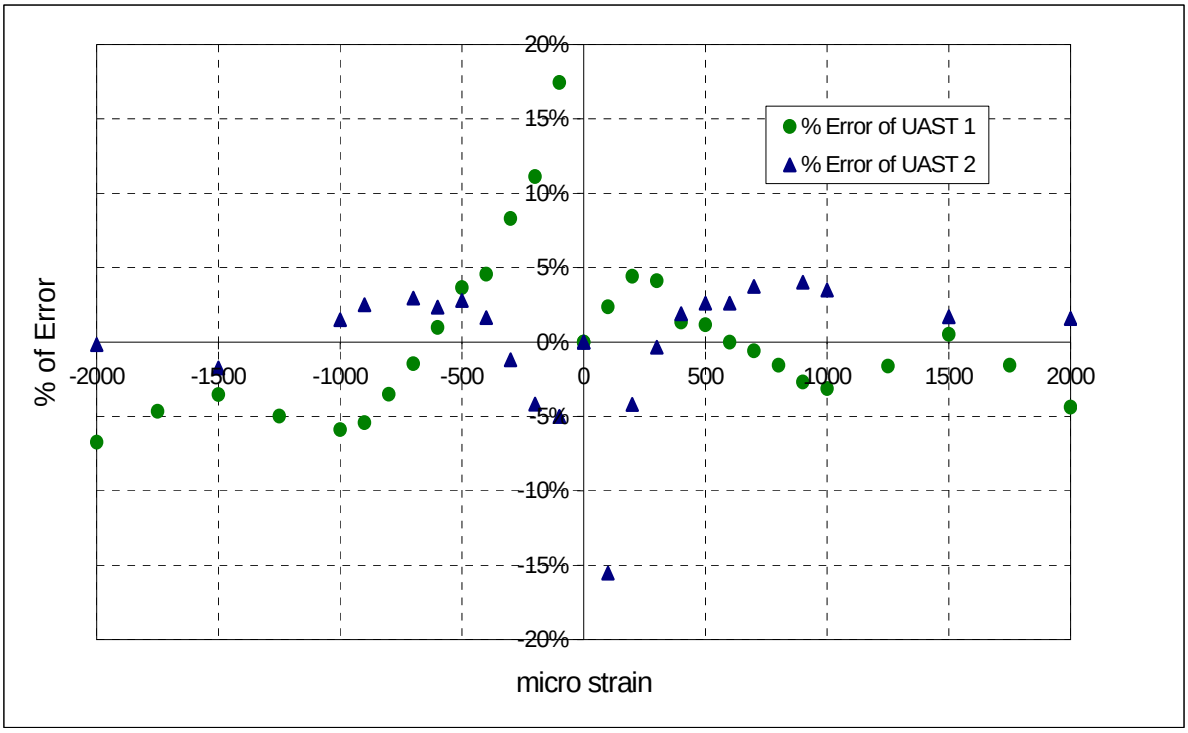


**Figure 5. Standard deviations of 20 measurements by UAST at various strain levels (UAST 1 and 2).**

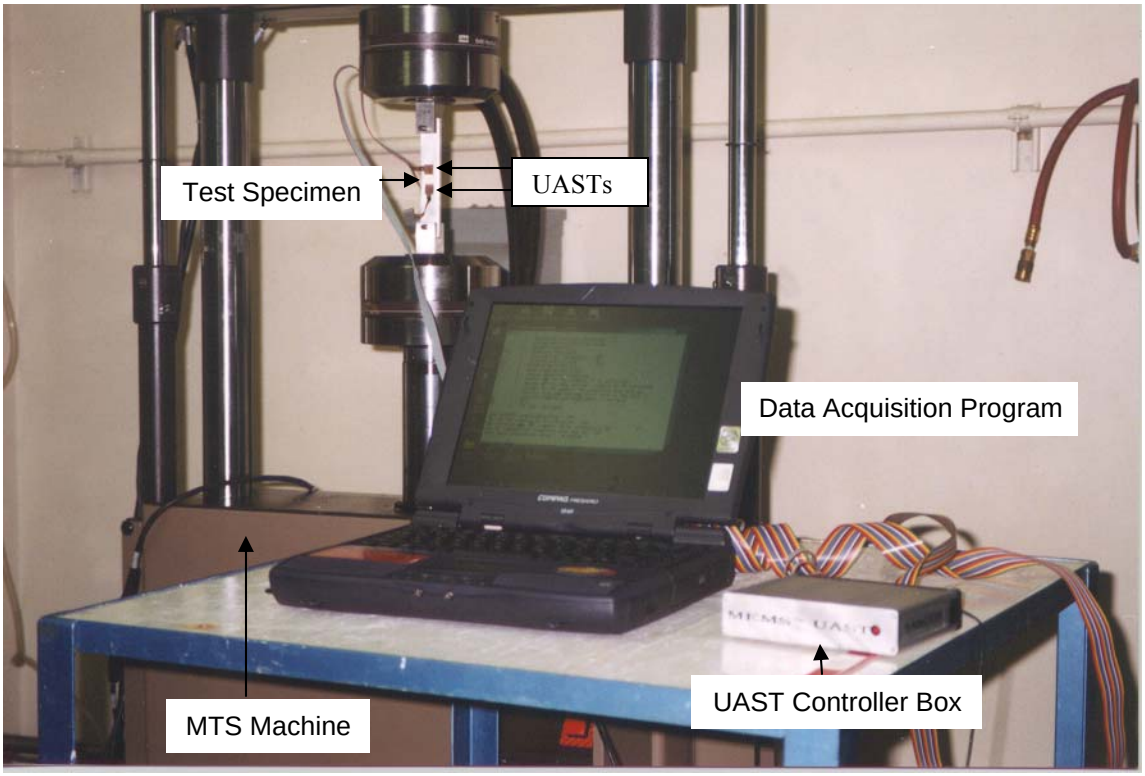


**Figure 6. Schematic of Laboratory Test Setup of Cyclic Loading Test**

**Table 4. Averages and Standard Deviations for Peak Strain Measurements**

| 12 Bit Mode (με) | | | | | | | | |
|---|---|---|---|---|---|---|---|---|
| 1 | | 2 | | 3 | | **Total** | | Resolution |
| AVG. | STD. | AVG. | STD. | AVG. | STD. | **AVG.** | **STD.** | 2.81 |
| 659.94 | 0.68 | 652.27 | 1.69 | 648.42 | 1.30 | **653.54** | **5.86** | |
| 13 Bit Mode (με) | | | | | | | | |
| 1 | | 2 | | 3 | | **Total** | | Resolution |
| AVG. | STD. | AVG. | STD. | AVG. | STD. | **AVG.** | **STD.** | 1.40 |
| 645.47 | 0.73 | 639.63 | 1.65 | 636.81 | 1.28 | **640.64** | **4.42** | |
| 14 Bit Mode (με) | | | | | | | | |
| 1 | | 2 | | 3 | | **Total** | | Resolution |
| AVG. | STD. | AVG. | STD. | AVG. | STD. | **AVG.** | **STD.** | 0.70 |
| 631.49 | 0.70 | 627.44 | 0.85 | – | – | **629.47** | **2.86** | |

| 15 Bit Mode (με) | | | | | | | | |
|---|---|---|---|---|---|---|---|---|
| 1 | | 2 | | 3 | | **Total** | | Resolution |
| AVG. | STD. | AVG. | STD. | AVG. | STD. | **AVG.** | **STD.** | 0.35 |
| 634.20 | 5.48 | 620.48 | 3.87 | 63.79 | 1.50 | **622.82** | **10.40** | |

**Table 5. Averages and Standard Deviations for Valley Strain Measurements**

| 12 Bit Mode (με) | | | | | | | | |
|---|---|---|---|---|---|---|---|---|
| 1 | | 2 | | 3 | | **Total** | | Resolution |
| AVG. | STD. | AVG. | STD. | AVG. | STD. | **AVG.** | **STD.** | 2.81 |
| 94.64 | 0.73 | 88.38 | 2.21 | 90.07 | 2.74 | **91.03** | **3.24** | |
| 13 Bit Mode (με) | | | | | | | | |
| 1 | | 2 | | 3 | | **Total** | | Resolution |
| AVG. | STD. | AVG. | STD. | AVG. | STD. | **AVG.** | **STD.** | 1.40 |
| 100.11 | 0.46 | 96.58 | 0.97 | 96.23 | 1.73 | **97.64** | **2.15** | |
| 14 Bit Mode (με) | | | | | | | | |
| 1 | | 2 | | 3 | | **Total** | | Resolution |
| AVG. | STD. | AVG. | STD. | AVG. | STD. | **AVG.** | **STD.** | 0.70 |
| 111.54 | 0.81 | 109.76 | 0.46 | – | – | **110.65** | **1.26** | |
| 15 Bit Mode (με) | | | | | | | | |
| 1 | | 2 | | 3 | | **Total** | | Resolution |
| AVG. | STD. | AVG. | STD. | AVG. | STD. | **AVG.** | **STD.** | 0.35 |
| 142.95 | 0.78 | 127.78 | 6.19 | 127.21 | 0.72 | **132.65** | **8.93** | |

**Table 6. No. of Data Points Collected per Loading Cycling**

| Modes of UAST | Data points at 9 HZ (15 mph) | Data points at 36 HZ (60 mph) | Data points at 72 HZ (120 mph) | Resolution |
|---|---|---|---|---|
| 12 bit mode | 106 | 26.5 | 13.25 | 2.81 με |
| 13 bit mode | 57 | 14.25 | 7.125 | 1.40 με |
| 14 bit mode | 33 | 8.25 | 4.125 | 0.70 με |
| 15 bit mode | 13 | 0.25 | 0.125 | 0.35 με |

## FATIGUE MODELING

There are a number of accumulative-damage monitoring algorithms that could prove viable as a means of recording the strain cycling history at a given location on a structural member to which a UAST is mounted. The objective of this task is to identify an algorithm with minimal data storage requirements within the sensor and to program it into the Programmable Integrated Circuit (PIC).

First, a set of strain threshold "bins" were defined across the dynamic range of the UAST device (e.g., every 500 micro-strain between -5000 and +5000 for the UAST). The UAST would then monitor the strain level it calculated after each sampling and determine whether the value had increased or decreased enough to place it into an adjacent bin—i.e., each departure from or entry into a bin would add one count to that bin. A histogram of this binning process could provide a basis for extracting out the cumulative strain cycling in terms of both strain magnitude and number of cycles. These data would then be used to assess remaining fatigue life, or as a means of documenting spurious overload conditions on a particular structural member.

### RAILROAD BEAM ON ELASTIC FOUNDATION

To estimate the stress and strain levels in a rail, a metal beam on an elastic concrete foundation was analyzed using the theory of mechanics. The railroad industry uses steel rails (E = 200Gpa) with a depth of 184 mm. The distance from the top of the rail to its centroid is 99.1 mm, and the moment of inertia of the rail is $36.9 \times 106$ mm$^4$. The rail is supported by ties, ballast, and a road bed that together are assumed to act as an elastic foundation with spring constant $k = 140$ N/mm$^2$. Or, the rail is assumed to be supported by concrete that is assumed to act as an elastic foundation with the same spring contant. As shown in Figure 7, it is assumed that a diesel locomotive has three wheels per truck, equally spaced at 1.70 m. The objective is to determine the maximum deflection, maximum bending moment, and maximum flexural stress in the rail if the load on each wheel is 170 kN.

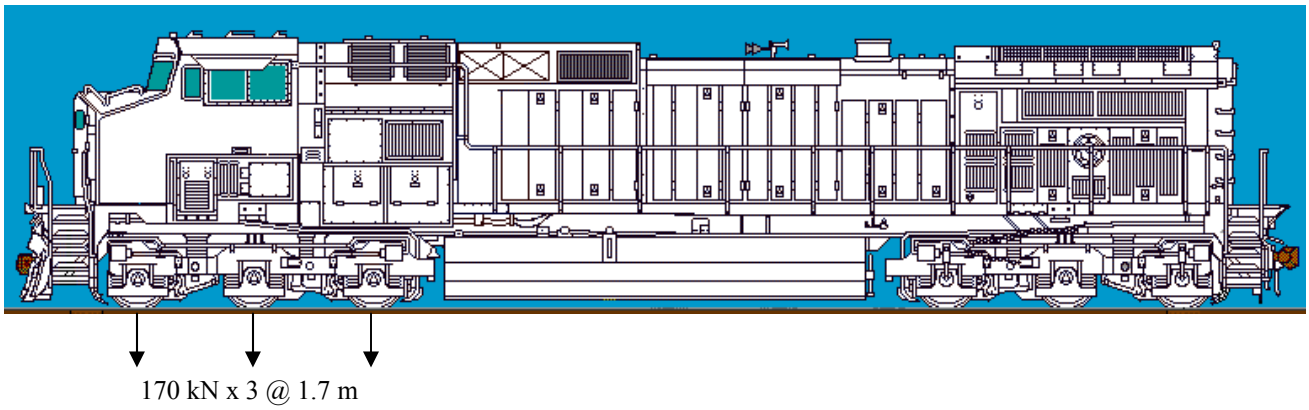


**Figure 7. A Diesel Locomotive with Three Wheel Loads of 170 kN each**

$$\beta = \sqrt[4]{\frac{k}{4EI_x}} = \sqrt[4]{\frac{140}{4 \cdot (200 \times 10^3)(36.9 \times 10^6)}} = 0.001476\, mm^{-1}$$

The deflection and bending moment at any section of the beam can be obtained by superposition of the effects of each of the three wheel loads. With superposition, the maximum deflection and maximum bending moment occur either under the center wheel or under one of the end wheels. Let the origin be located under one of the end wheels. The distance from the origin to the next wheel is $z_1 = 1.7 \times 10^3$mm. Hence, $\beta z_1 = (0.001476)(1.7 \times 10^3) = 2.50$. The distance from the origin to the second wheel is $z_2 = (2)(1.7 \times 10^3)$mm. Hence, $\beta z_2 = (0.001476)(2)(1.7 \times 10^3) = 5.00$.

Based on a rail mechanics theory, the following constants are obtained:

$$A_{\beta Z1} = -0.0166, \qquad C_{\beta z1} = -0.1149$$
$$A_{\beta Z2} = -0.0046, \qquad C_{\beta z2} = 0.0084$$

The deflection and bending moment at the origin (under one of the end wheels) are then computed as:

$$y_{end} = \frac{P\beta}{2k}(A_{\beta z0} + A_{\beta z1} + A_{\beta z2}) = 0.8961(1 - 0.0166 - 0.0046) = 0.877 mm$$
$$M_{end} = \frac{P}{4\beta}(C_{\beta z0} + C_{\beta z1} + C_{\beta z2}) = 28.79 \times 10^6 (1 - 0.1149 + 0.0084) = 25.72 kN \cdot m$$

Now, let the origin be located under the center wheel. The distance between the center wheel and either of the end wheels is $z_1 = 1.7 \times 10^3$mm. Therefore,

$$y_{center} = \frac{P\beta}{2k}(A_{\beta z0} + 2A_{\beta z1}) = 0.8961\left[1 + (2)(0.0166)\right] = 0.926 mm$$
$$M_{center} = \frac{P}{4\beta}(C_{\beta z0} + 2C_{\beta z1}) = 28.79 \times 10^6 \left[1 + (2)(-0.1149)\right] = 22.17 kN \cdot m$$

Thus,

$y_{center} = y_{\max} = 0.926 mm$,
$M_{end} = M_{\max} = 25.72 kN \cdot m$,
and

$$\sigma_{\max} = \frac{M_{\max} c}{I_x} = \frac{25.72 \times 10^6 \times 99.1}{36.9 \times 10^6} = 69.1 MPa$$
$$\varepsilon_{\max} = \frac{\sigma_{\max}}{E} = \frac{69.1 \times 10^6}{200 \times 10^9} = 346 microstrains$$

## CYCLE COUNTING ALGORITHMS

A number of cycle counting algorithms have been developed in the past. The peak count method identifies the occurrence of relative maximum or minimum load values by counting peaks above the reference load level and valleys below the reference load. Normally, the peak count method constructs the largest possible cycle using the highest peak and lowest valley, followed by the second largest cycle constructed in same manner. In contrast, the peak-between-mean crossing count method only counts the largest peak and valley between successive crossings of the mean.

In the level-crossing count method, one count is registered whenever the strain exceeds a preset level; the count is positive if it is above the reference strain and negative if it is below the reference strain. The restricted level crossing count is similar to the level crossing count except that only one count is made between successive crossings, or a lower level associated with each counting level. Like the peak count method, the level-crossing method must be rearranged by counting peaks above the reference strain and counting valleys below the reference strain. For the range count method and range-mean count method, a range is defined as the difference between two successive reversals. The range becomes positive when a valley is followed by a peak, and negative when a peak is followed by a valley. Both positive and negative ranges are counted as half cycles. When small reversals are counted, the range and range-mean count methods break up a large range into several smaller ones. Thus, it may give unrealistic results in that a large cycle may go unrecognized where smaller cycles are superimposed.

The rain flow method is one of the most widely used counting methods. Several rules are imposed on the rain flow method to define cycles and half cycles. Before applying the rain flow method, an accurate strain-time history has first to be obtained. If small amplitude ripples of cyclic strain are counted as peaks and valleys, the method may over-estimate the number of loading cycles. Therefore, a filtering technique has to be used to remove those noises first. If a small amplitude ripple is less than a filter magnitude, it will not be counted as a peak or valley.

## CUMULATIVE DAMAGE MODELING METHODS

Many cumulative damage modeling methods have been proposed in the past (Gatts 1961). Among these methods, Palmgren-Miner's hypothesis is one of the most frequently used due to its simplicity and relatively high accuracy (Miner 1945). As illustrated in Figure 8, Equations (1) to (3) can be used to apply Palmgren-Miner's hypothesis.

$$D_i = \frac{n_i}{N_i} \qquad \textbf{(1)}$$

$$D_1 + D_2 + \cdots + D_{i-1} + D_i \geq 1 \qquad \textbf{(2)}$$

$$\sum_{j=1}^{i} \frac{n_j}{N_j} \geq 1 \textbf{. (Failure Criteria)} \qquad \textbf{(3)}$$

where, $D_i$ = damage fraction
$n_i$ = number of cycles applied at stress amplitude $S_i$
$N_i$ = the number of cycles of completely reversed stresses $S_i$ to produce failure.

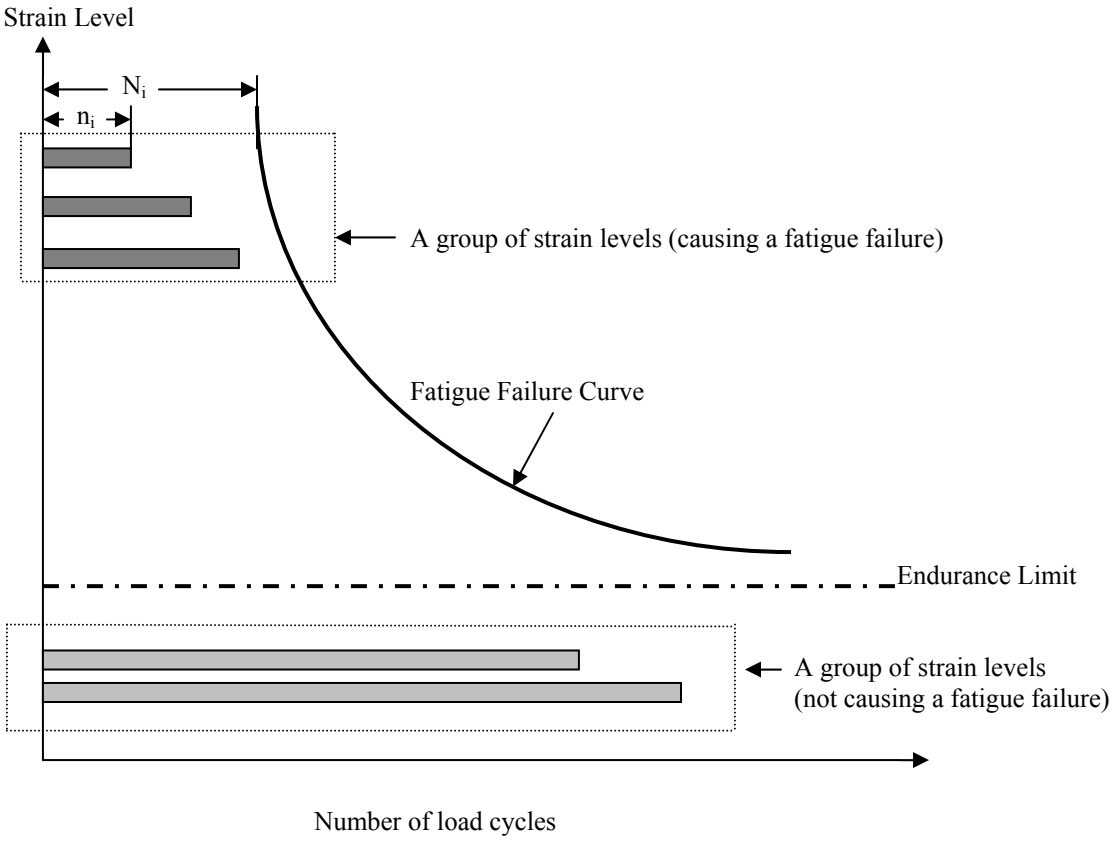


**Figure 8. Rail reaching its fatigue life (Palmgren-Miner's hypothesis).**

## PROTOTYPE HYBRID UAST

A design of a prototype Hybrid UAST was completed, integrating the basic functionality of the UAST with 1) the logic necessary to implement the binning algorithm, 2) the use of non-volatile RAM to store the processed data, 3) modifications to the UAST communication port to provide periodic downloading of the data sets, and 4) other aspects related to network-specific power distribution and local clock generation. The integrated design and binning algorithms were validated using programmable logic and standard packaged integrated circuits. The successful fabrication of the prototype Hybrid UAST set the stage for future hybridization of the UAST sensor package to include all of the operational functions in as small a volume as possible. The prototype Hybrid UAST consists of three parts: the UAST (sensor), the networking controller box, and the communication cable. Figure 9 shows a schematic design of the battery operated Hybrid UAST controller. A cycle counting algorithm was integrated into the Programmable Integrated Circuit (PIC) micro-controller, which is programmable using a set of configuration switches.

With traditional data acquisition systems, it is extremely difficult to conduct long-term fatigue tests because these sensors need massive signal processing devices, power source, wiring, etc., and such electric devices are not durable. Therefore, to monitor infrastructures in remote locations, the portability of testing devices is particularly important. The small storage device and on-chip signal processing features make the Hybrid UAST extremely portable testing device. And unlike a traditional permanent testing setup, with the Hybrid UAST once a test has been completed at a testing site, the same sensors can be easily reused at the next spot.

### CONTROLLER BOX

#### Configuration

As shown in Figure 10, there are three switches on the right-hand side of the controller box. When the switch is up, it is in the ON position (or in state 1). Looking at the panel in Figure 10, from the bottom up on the right-hand side, the switches have the following functions.

*Switch 1: Mode Switch 1 = Acquisition Mode, 0 = Command Mode*

When the switch is 1 (or up), the UAST sensor is in acquisition mode and is collecting data at a fixed frequency depending on the resolution. If the PC is connected and binning is turned on, raw data can be viewed on screen and saved to a disk. When the switch is 0 (or down), the UAST is in command mode. In this mode, the controller is waiting to transfer bin data to the PC.

*Switch 2: Resolution Switch 1 = 14 bit mode, 0 = 12 bit mode.*

This switch is only read at power up or reset, and it sets the fixed sample rate and resolution of the UAST sensor. The sampling rates of resolution modes are: 953 samples/sec for 12-bit mode (1.05 ms per sample), and 284 samples/sec for 14-bit mode (3.52 ms per sample).

*Switch 3: Binning Switch 1 = Binning ON, 0 = Binning OFF*

This switch, when ON, passes the raw data to the binning algorithm to be processed. If the switch is OFF, the bins remained unchanged even if an acquisition is currently running. The switch also serves another purpose, which is to synchronize the raw data with the binning algorithm. When a raw data acquisition has been started by a computer's data collection software, the computer waits until the binning switch goes to the "up" position to actually collect the data. To stop the acquisition, the binning switch can be turned off. The data can then be written to a file with a command from the data collection software.

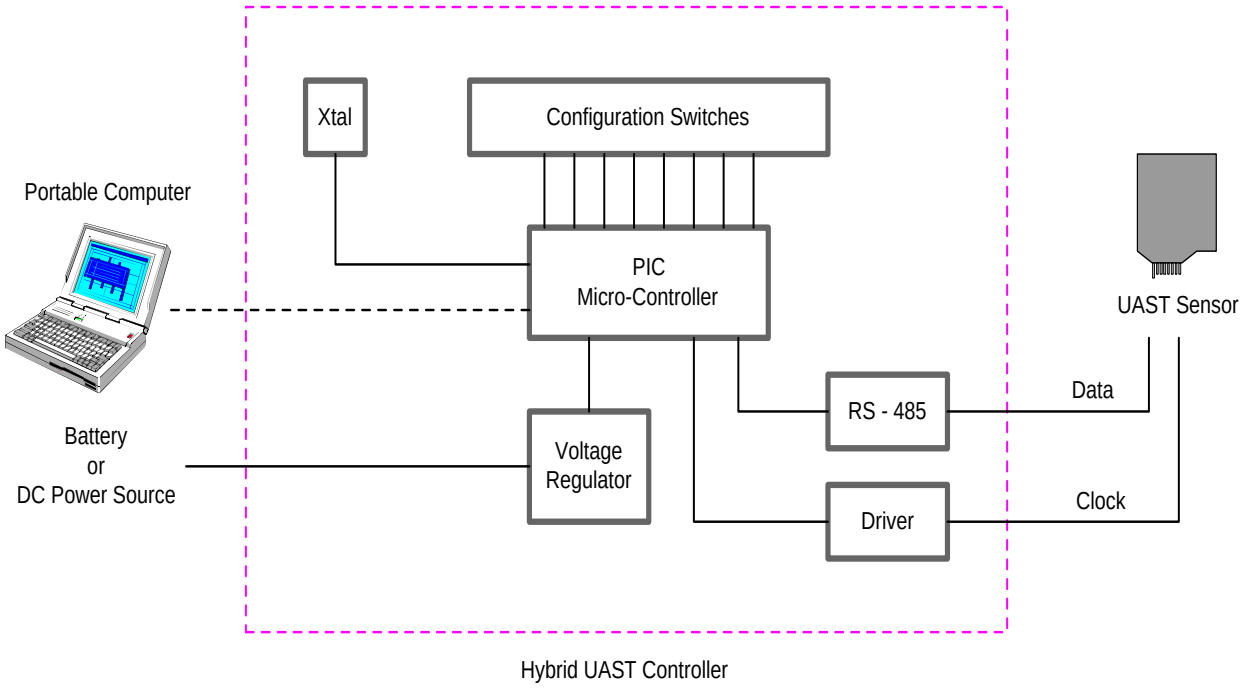


**Figure 9. Schematic design of Hybrid UAST Controller.**

**Figure 10. Controller box connected to two UAST's on a rail.**

**Operating Instructions**

The computer is just an observer, and, therefore, the acquisition and data collection happens regardless of the connection status of the computer. As discussed earlier, the controller's action is based on the setting of the switches on the right-hand side panel. Upon power up (or reset), the controller takes 64 samples of data and calculates a mean value as the starting point for the binning. All data points binned after startup will be measured as a relative displacement from the mean. If a new mean is desired, a power cycle (or reset) is required. The basic set-up and typical operation procedure are described below.

1) Plug 9V 500mA regulator or 4 AA regular alkaline batteries with the appropriate power connector into the controller box.
2) Make sure the power switch on controller box is off. (LED out).
3) Plug the UAST and cable assembly into the DB-9 of the controller box.
4) Plug the parallel port cable into the PC and controller box (for data acquisition).
5) Turn on the power to the controller box using power switch.
6) Run the data acquisition software on a PC.
7) Set the binning switch OFF.
8) Set the mode switch to acquisition and then press the reset button (to set a new mean value).
9) Select option "c" from the data acquisition software to collect data (software notifies that it is waiting for an acquisition to start).
10) Turn the binning switch ON.
11) When acquisition is done, turn the binning switch OFF.
12) Select option "f" from the data acquisition software to write raw data to a file.
13) Change the mode switch to command mode.
14) Write collected bins to a file.

**DATA ACQUISITION SOFTWARE**

As shown in the main menu (see Figure 11), a data acquisition software package was developed to 1) display raw data, 2) display bins, 3) collect raw data, 4) write raw data to a file, and 5) write bin data to a file. There is a parameter file with

three values that the user can easily change. The first is a file number for bin data, the second is the file number for raw data, and the third is the size of the data buffer. The file number increments after each data set, allowing the user to take multiple sets of data for later analysis. The data buffer determines how long raw data can be collected continuously to the computer. The software can be started and stopped completely independently of the controller box. Again, the computer and the data acquisition software are just observers of the controller.

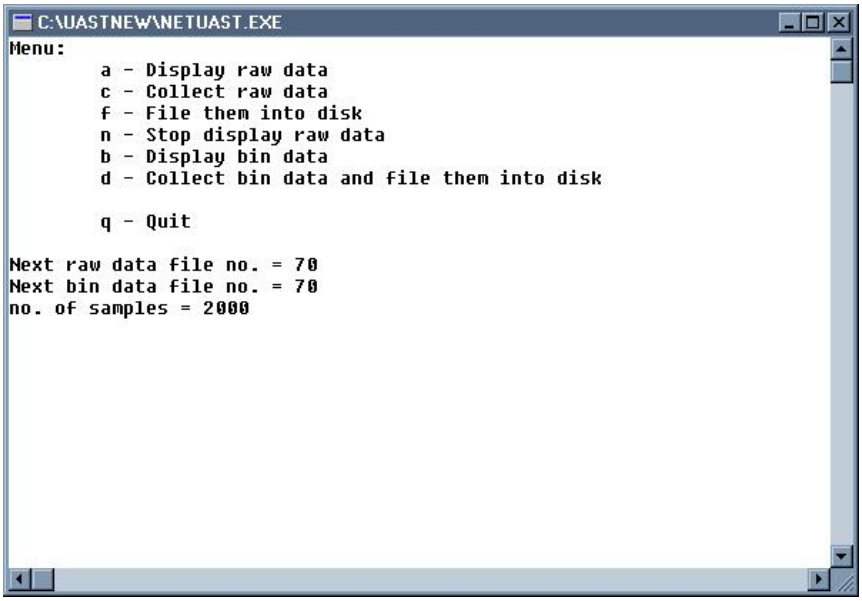


**Figure 11. A computer window screen of a main menu of the data acquisition software package.**

## DATA ANALYSIS SOFTWARE

Another software package was developed to process the raw data from a computer so that the binning result from the controller box can be compared for their accuracy. The PICs now process results into ten bins between +400 UAST counts and -1600 counts (1 count = 0.35 με) relative to the starting mean (i.e., filter magnitude and bin width both equal 200 counts). The software can find peaks and valleys following the predetermined filter magnitudes, it can display peak/valley data, and write bin data to a file. It can also post-process both the raw data files and the binning data downloaded from the PIC. This will allow independent calculation of the binning results from the raw data, as well as the "reconstruction" of the peaks and valleys either from the raw data or from the PIC-reported binning results. The calibration constants must be applied to convert "counts" into "micro-strain" since this will depend on which type of sensors is used. The conversion values for these constants are 0.35 με per count for the old UAST devices (without mounting stems) and 0.25 με per count for the new UAST devices (with mounting stems).

This software package can be used to process the strain data measured from a rail in the field. As shown in the main menu (see Figure 12), the "Read Raw File" button allows the user to select and read in a raw data file. The number of samples read will be displayed next to the sample size label. It should be used in conjunction with the "Calc All" button shown at the bottom left of the computer screen (do not use the "Calc PV" button with this mode). If the "Use Mean" button has been checked, the "Calc All" button will use the value entered below the "Use Mean" button for the mean calculation and offset. If the "Use Mean" button has not been checked, as the file is being read in the "Read Raw File" option, the program will calculate the mean from the first 64 data points in the raw data file.

The "Read Bin File" button allows the user to select and read in a bin file generated from the controller box described above. This button is used in conjunction with the "Calc PV" button only. The "Reset" button returns variables to their initial, start-up state. Use this button before reading in a “Raw” or “Bin” file using the "Read Raw File" button shown on the computer screen. The "Write Files" button writes out the output files after a "Calc All" or a "Calc PV" has been completed. Three files are created by this function. The first file is "RawXXX.out," which contains the

computational results displayed in the main window as shown in Figure 12. The second file, "RawXXXBins.out," is a table of the bin counts arranged in 10 rows and 10 columns. The last number in the file is the mean used to generate the bin results. Finally, the 3rd file, "RawXXXPV.out," is a reconstruction of the estimated original peaks and valleys. This file is generated based on the contents of the "RawXXXBins.out" file.

The "Calc All" button computes the bins from the raw data file and uses them to generate a peak and valley reconstruction. This function can be used only in conjunction with the "Read Raw File" button. The "Calc PV" button computes the reconstructed peaks and valleys from a bin file read using the "Read Bin File" button. If the "Use Mean" button is not selected, the "Print Stats" button prints out the max, mid, mean, min, and a mean of the first 64 data samples of the raw data set (if the "Use Mean" button is selected, the numbers it reports are meaningless). The "Print Bins" button displays the calculated bin data. After a "Calc All" procedure, this will display on the main window, which will be written to the "RawXXXBins.out" file. The "Print Data" button displays on the main window the first 70 raw data points from a file that was read using the "Read Raw File" button. The "Print PV" button displays the reconstructed peak and valley data on the main window. Finally, the "Clear" button clears the main window display.

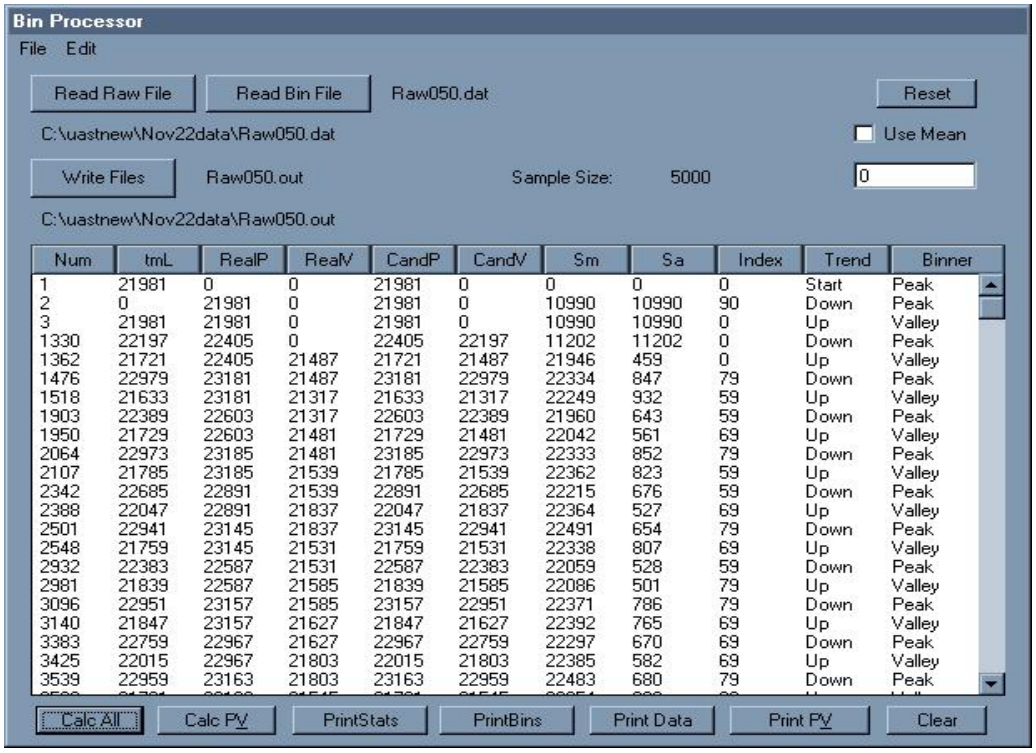


**Figure 12. A computer window screen of a main menu of the binning software package**

## FIELD TESTING OF PROTOTYPE HYBRID UAST

As shown in Figure 13, actual UAST strain data were taken from test rail sections in Salt Lake City and Iowa City. The collected strain data were processed using the software packages discussed in the previous section. These software packages were used to find the peaks and valleys from a series of strain data and the subsequent binning operation. They were successfully implemented in a co-located battery-operated controller box as shown in Figure 13.

## FIELD DATA COLLECTION

Several attempts were made to collect strain gauge data from the rail structure in the field from July through December, 1999. All devices were tested indoors and they were deployed in the field. When we tested them indoors, they always worked well, but when we took them outside for field testing, at the beginning, they did not work properly. Eventually, it worked very well and we set up the data acquisition system in the field. A cause for a temporary malfunction remains to be determined. We used two different Programmable Integrated Circuits (PIC) for the controller because we had two different types of UASTs, one with a mounting stem and the other without. We concluded that the Hybrid UAST developed from this research must be recognized as a prototype device intended for evaluation purposes only; it has not been "weatherized" or "ruggedized" in its present form. However, the device was evalauated at the less than ideal situation. As a matter of fact, it was a challenge to mount the device at the bottom of the rail due to the accumulated and compacted soil under the rail beam.

Another observation we made during the field testing was that the rail structure was in a very poor condition. The rail head was cracked and some of them were broken. Wooden ties were severely weathered and damaged to the extent that the fasteners attaching to the rail could become loose. It was also very difficult to mount the UAST under the rail because there was no gap between the rail and the ballast bed as originally expected. The base of a rail was buried in the soil accummulated on top of the ballast. It left no room for installing the UAST. Therefore, we had to dig under the rail to create a space to install the device. In another incident, a connector wire to the UAST was severely damaged due to loose rocks and was later repaired. It is clear that the packaging of the UAST and its wiring and connectors must be improved to survive the outdoor rail environment for long-term use.

## FIELD DATA ANALYSIS

Figure 14 shows a set of 5000 raw data points collected from the bottom of a rail without a train at the frequency of 290 Hz (12-bit mode of UAST) for 17.24 seconds. This figure illustrates the repeatability of the strain data collected using a Hybrid UAST from the rail without a load. As can be seen from the figure, almost all observations were within 4 microstrains without any loading. With no load on the rail, a standard deviation of strain measurements was 1.25 microstrains, which means that 95% of the measurements were no more than 2.5 microstrains. Figure 15 shows another set of 5000 raw data points collected from a rail with a train at the same frequncy. The data clearly indicate locations of the peaks and valleys due to the bending and compression stresses caused by a running train. As shown in Figure 15, tensile strain values were consistently measured up to 400 microstrains, which are quite reasonable according to the theoretical calculations discussed earlier. They are also very similar to a typical set of strain data collected from other rail test tracks (reference to be included here). The strain signatures from a train load are distinctively clear, with easily identified peaks and valleys for a fatigue analysis. Figure 15 clearly shows two peaks caused by dual axles of a train and an intermediate peak between two axle peaks, which might have been caused by the closely spaced axle loads. Appendix A presents four additional sets of raw data collected from a rail under a trainload in the field, which are quite similar to Figure 15. Although the magnitudes of the trainloads were not known in the field, their loading patterns including the peak values are quite consistent with each other. Their peak strain values were not expected to be the same because they were measured from the different trains. However, the similar patterns of the strain values with a reasonable range of minimum and maximum values support the repeatability of the prototype Hybrid UAST.

**Figure 13. Strain data collection from a rail using UAST™ and a controller box.**

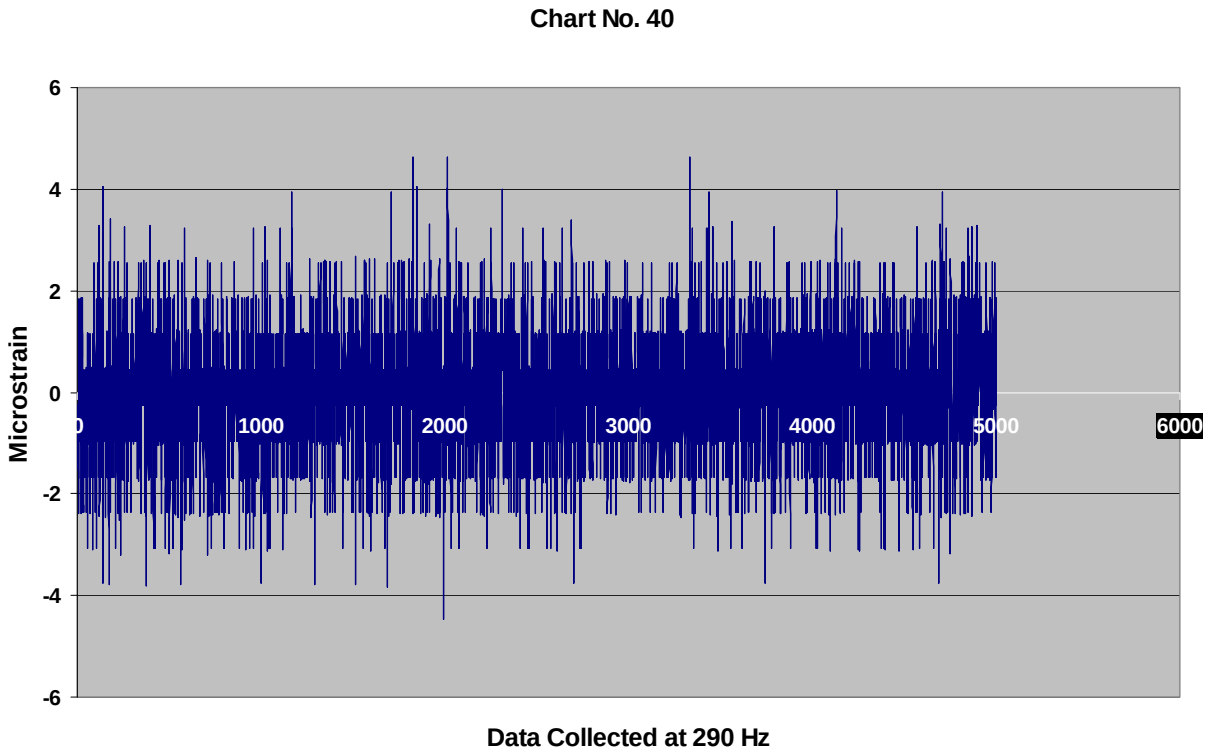


**Figure 14. Typical UAST measurements from rail without a train in the field.**

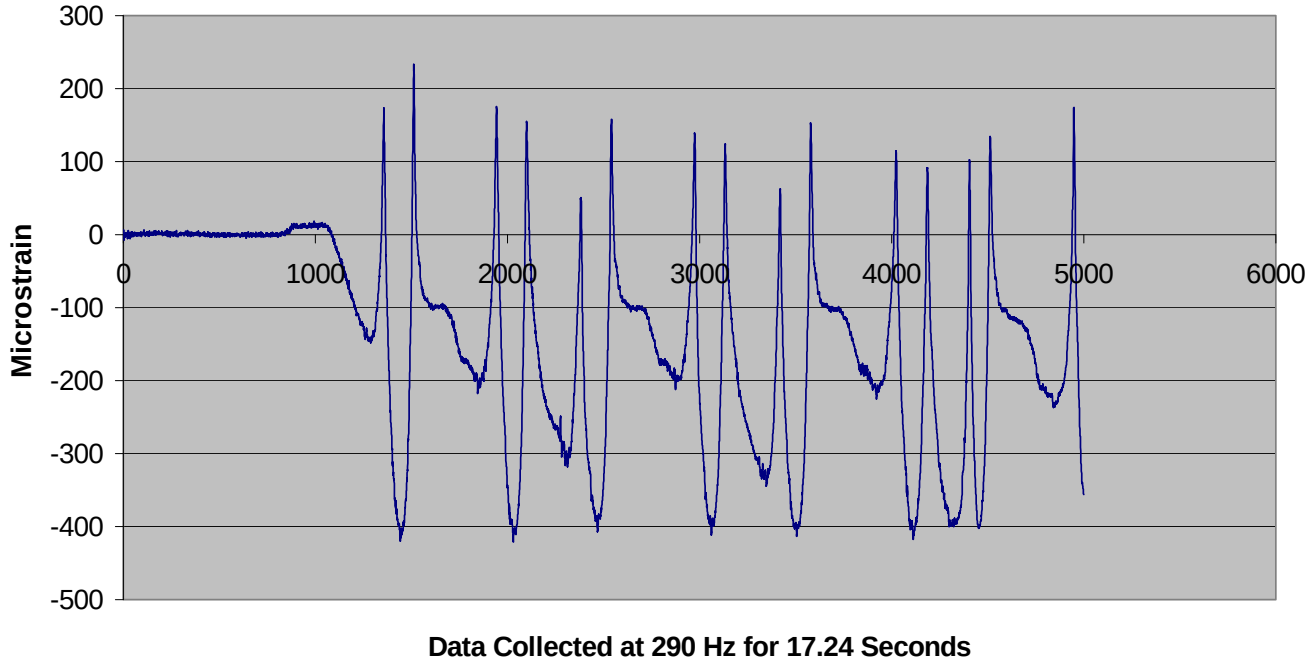


**Figure 15. Typical UAST measurements from rail with a train in the field**

To convert these data points into micro-strain, the raw digital UAST data were first zeroed about the starting mean of 64 counts and a calibration constant of 0.35 was applied. Using the cycle counting software called "Binner," the load cycles were counted with a filter magnitude (25 micro-strain in this case) to identify the peaks ("o") and valleys ("x"). The binning results from the algorithm can be downloaded from the processor, representing the number of 1/2-cycles counted within the range of each combination of mean strain and cycle amplitude. As shown in Figure 16, reconstruction of the peaks and valleys can then be easily accomplished using the "Binner" software package. Figure 17 shows these load cycle counting results downloaded from the microcontroller with the peaks and valleys reconstructed from the compiled data.

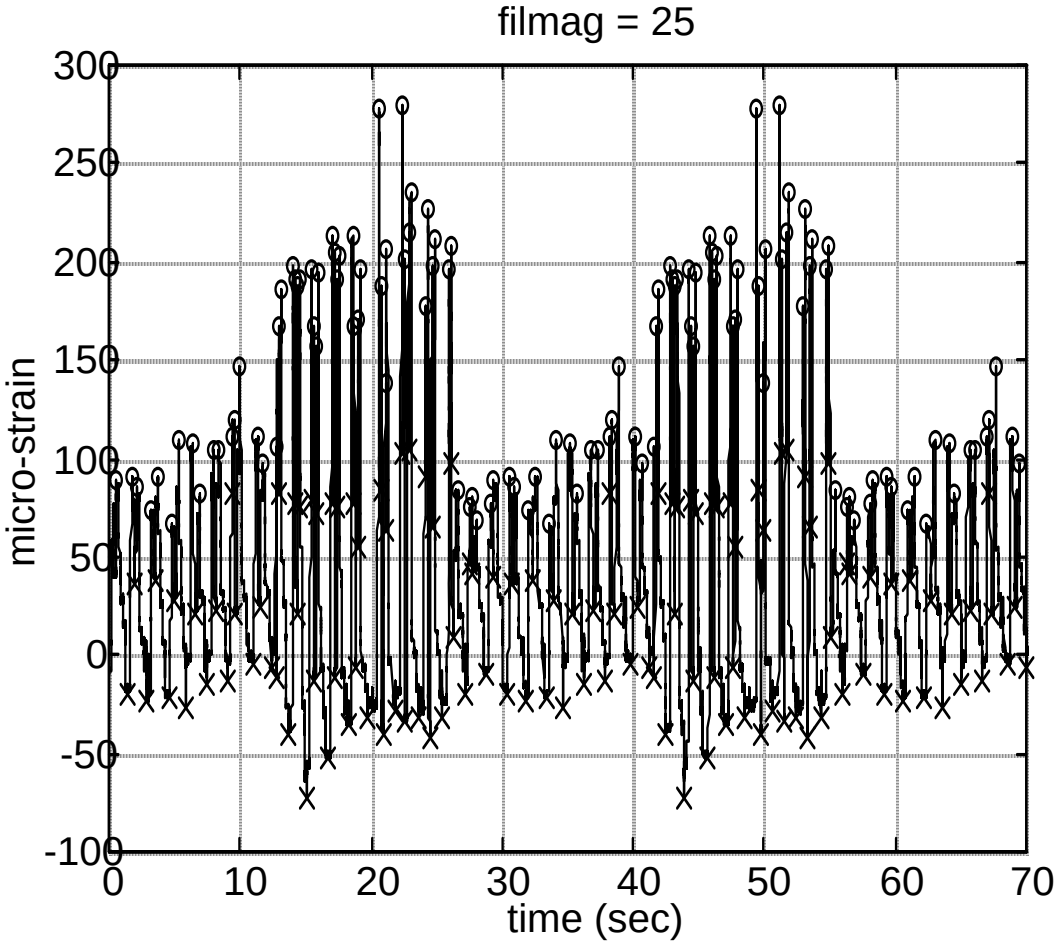


**Figure 16. Raw digital UAST data (shown above) and micro-strain (shown below) with the detected peaks ("o") and valleys ("x").**

```
                                                                    == increasing mean strain ==>
                 0     0     0     0     0     0     0     0     0     0
                 0     0     0     0     0     0     0     0     0     0
                 0     0     0     0     0     0     0     0     0     0
                 0     0     0     0     0     0     2     2     0     0
                 0     0     0     0     4     4     2     0     0     0
                 0     0     0     0     8    24     0     0     0     0
                 0     0     0     2     5     8     6     0     0     4
                 0     0     0    36     3     3     2    34     8     0
                 0     0     3    15    30     0    10     4     2     0
                 0     0     0     3    20     3     3     0     0     0
== increasing
  amplitude ==>
```

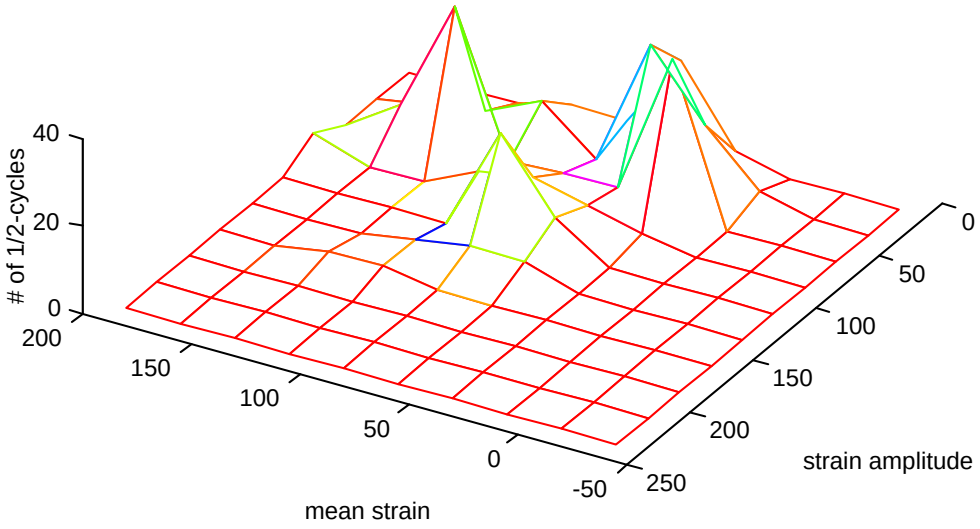


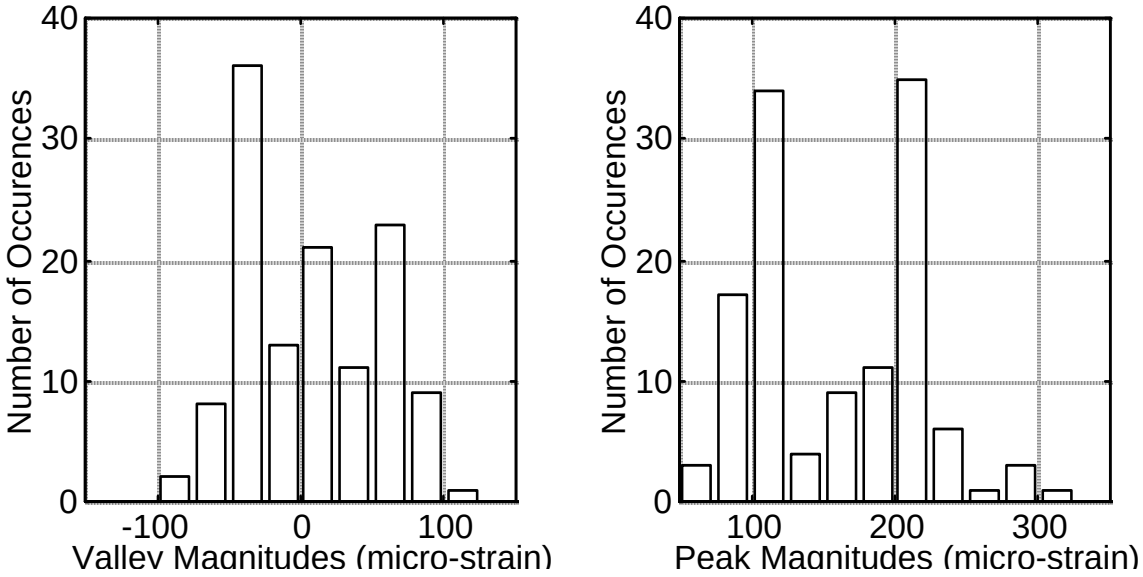


**Figure 17. Frequency plots of binning results from the cycle counting algorithm.**

## PLANS FOR IMPLEMENTATION

As stated earlier, the Hybrid UAST developed from this Type 1 project is a prototype device intended for evaluation only and has not been "weatherized" or "ruggedized". It is a simple laboratory prototype, which needs to be developed further for a commercial-grade device. It was also reported that, during testing, a connector wire to the UAST was damaged and had to be repaired. Thus, the packaging of the UAST and its wiring and connectors should be improved to survive the outdoor rail environment for long-term use. As demonstrated in the report, it will be possible to manufacture a commercial-grade of Hybrid UAST for implementation in the field. However, more extensive field investigation of the Hybrid UAST and a rigorous analysis of the field results are critically needed to enhance the potential for developing a production version of the sensor.

This Type 1 project has proven the feasibility of developing a prototype Hybrid UAST, with positive results from both laboratory and field tests. Therefore, we are currently seeking continued supplemental resources from the TRB-IDEA Program to investigate the transfer of the Hybrid UAST technology to users and its application in practice (with a significant amount of matching funds from the University of Iowa, Sarcos Research Corp. and the Association of American Railroads).

## CONCLUSIONS

This research sought to determine the potential of the Hybrid UAST to continuously monitor, analyze, and store the strain history of components such as rail. To store strain cycling history, we developed a prototype Hybrid UAST, which includes non-volatile RAM. The prototype Hybrid UAST consists of three parts: a UAST sensor, a networking controller box and a communication cable. The data acquisition program was developed to operate the Hybrid UAST from a laptop computer. The data analysis program was then developed to implement the peak searching and cycle counting algorithms into the programmable microcontroller.

Laboratory tests using an aluminum beam installed with UASTs and conventional foil strain gauges demonstrated the accuracy and repeatability of the UASTs. A series of cyclic loading tests was performed to evaluate the UASTs under a moving trainload applied on the rail using an MTS cyclic loading machine. Overall, these laboratory test results indicate that the UAST is accurate and repeatable in a wide range of strain values from 0 to 2,000με.

An optimum technique for mounting the UAST to rail was developed using separate, detachable mounting pads. A prototype Hybrid UAST package was then fabricated and tested in the field. Raw data were collected to verify the cycle counting algorithm implemented in the Hybrid UAST in an outdoor operating environment. The raw data collected at 290 Hz without a train consistently showed a standard deviation of around 1.25 με, where 99.7% of background noises are less than 3.75 με. This level of error can be considered small relative to a peak strain range of 400 με caused by a typical trainload. The raw data collected from a rail under the train were also processed by the Hybrid UAST to accurately determine not only the number of load cycles but also the magnitudes of the peak loads. They are consistent with both laboratory measurements and theoretical calculations. However, there were a few instances in which the prototype Hybrid UAST did not work outdoors, even though it had worked in the indoor laboratory. Although the prototype Hybrid UAST worked in the field eventually, we must stress that the fabricated hybrid UAST is a prototype device that has not been ruggedized in its present form.

A project panel meeting was held to review the project objectives and approach. The panel indicated that the proposed Hybrid UAST could be suitable for monitoring track and bridge structures at remote locations, and for estimating their remaining service life in the interest of maintenance planning. The panel proposed additional potential application areas, including a train presence detection device, wireless instrumented wheel sets, a portable weigh-in-motion device, and a device to predict buckling of the rail.

In conclusion, both laboratory and field testing of the prototype Hybrid UAST with respect to its repeatability, accuracy, and viability in hybridization can be considered a great success. We also conclude that the proposed Hybrid UAST is suitable for monitoring railroad and bridge structures at remote locations, and for estimating the remaining service life of structures for maintenance planning.

In the future, the performance of a networked set of Hybrid UASTs should be continuously monitored under load-controlled environment for a longer period of time, say one week. Strain data collected by the Hybrid UAST should be compared against the ones measured by traditional strain gauges along with temperature compensations. Additional research will be required to investigate the cause of the unexpected malfunction to improve the reliability. Therefore, we recommend that a series of robustness tests be conducted in a harsh environment like the winter and the summer in Iowa.

## INVESTIGATOR PROFILE

**Hosin Lee, Ph.D., P.E., Principal Investigator**

Dr. Lee is an associate professor in Civil and Environmental Engineering and Public Policy Center at the University of Iowa. He has served as a director for the Center of Excellence for Advanced Construction Materials at the University of Utah. He received a B.S. degree in 1980 from Seoul National University, an M.S. degree in 1981 from Stanford University, and a Ph.D. from the University of Texas at Austin in 1985, all in civil engineering. His publications include 20 papers in the area of transportation infrastructure, which have appeared in refereed journals such as ASCE, TRB and ASTM. He has served on the National Cooperative Highway Research Program (NCHRP) Advisory Panel, and has coordinated the National Highway Institute sponsored highway pavements courses. Dr. Lee was selected as an "Educator of the Year 1995" by the Utah Section of the ASCE, and "Engineering Educator of the Year 1996" by the Utah Engineers Council. He has also received an Eisenhower Faculty Fellowship from the National Highway Institute. He is a licensed professional engineer registered in the state of Utah, and a member of the technical national committee on pavements and highway materials in ASCE, TRB, and ASTM.

**Stephen C. Jacobsen, Ph.D.**

Dr. Jacobsen is a professor in Mechanical Engineering and a director of the Center for Engineering Design at the University of Utah. He received a B.S. degree in 1967 and an M.S. degree in 1970 from the University of Utah, and a Ph.D. from the Massachusetts Institute of Technology in 1973. A key innovator in developing dexterous and entertainment robots, teleoperation systems, and micro electro mechanical systems (MEMS), Dr Jacobsen currently holds over 90 U.S. and foreign patents. He has authored over 160 publications, and has received numerous awards for system design and innovation. Dr. Jacobsen is the president and chairman of the board of the Sarcos Research Corporation. He is a member of the National Academy of Engineering and the National Institute of Medicine.

**Brian J. Maclean, Ph.D.**

Dr. Maclean is a project leader in the MEMS group at the Sarcos Research Corp. and is currently involved in a number of sensor, actuator, and control aspects of smart structure research. These activities include sensor networks for health monitoring of aging aircraft and flow field measurements of aero/hydrostructures, development of adaptive airfoils, and active strengthening of columns under compressive loading.

## REFERENCES


Baker, M. A., "Semiconductor Strain Gauges", *Strain Gauge Technology*, Editor, Editor, Window, A. L. and Holister, G. S., Applied Science Publisher, LTD., NJ, 1982.

Charlmers, G. F., "Materials, Construction, Performance and Characteristics*", Strain Gauge Technology*, Editor, Window, A. L. and Holister, G. S., Applied Science Publisher, LTD., NJ, 1982.

Gandhi, M. V. and Thompson, B. S. Smart Materials and Structures, Chapman & Hall, UK, 1992.

Gatts, R. R., "Application of a Cumulative Damage Concept to Fatigue", *ASME Transactions*, Vol. 83, Series D, No. 4, 1961: 529.

Maclean, B.J., M.G. Miladejovsky, M.R. Whitaker, and M. Olivier, "A Digital MEMS-Based Strain Gage for Structural Health Monitoring," Proceedings of MRS Conference, Boston, December, 1997.

Miner, M. A., "Cumulative Damage in Fatigue", Journal of Applied Mechanics, (September, 1945), ASME, pp. A-159-A-164, .1945.

Neubert, H. K. P., *Instrument Transducers — An Introduction to their performance and design*, 2nd Edition, Oxford University Press, London, 1975.

Simpson, C. D., *Principles of DC/AC Circuits*, Englewood Cliffs, NJ, Prentice-Hall, Inc., 1996.

Yun, H.B., "Development of Hybrid Uni-Axial Strain Transducer for Transportation Infrastructure," M.S. Thesis, University of Utah, December 1999.

# APPENDIX A

Four Sets of Strain Data Collected at 290 Hz
from a Rail under a Train for 7.24 seconds

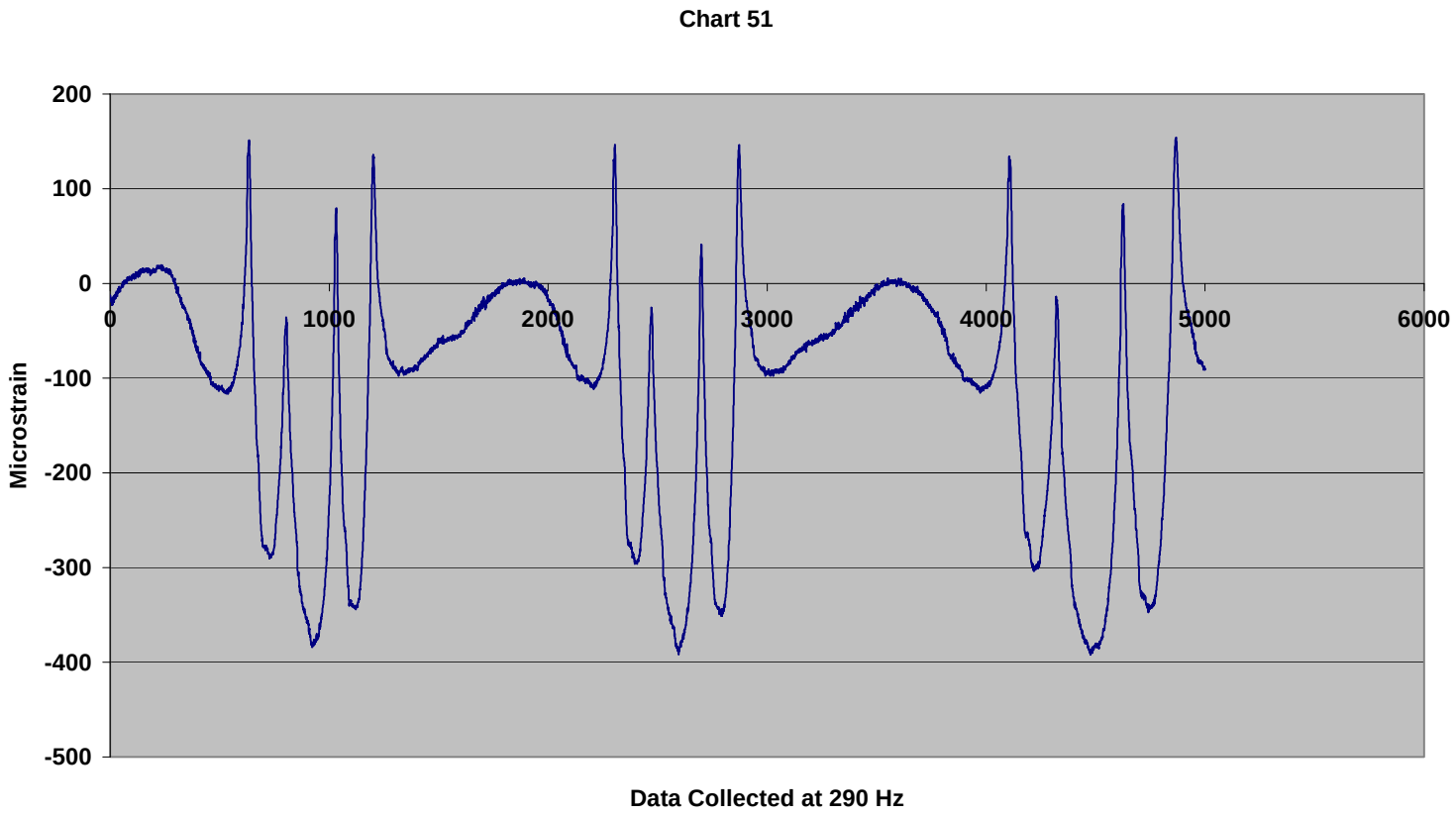


Figure A.1. Strain Data Collected from a Rail with a Train for 7.24 seconds

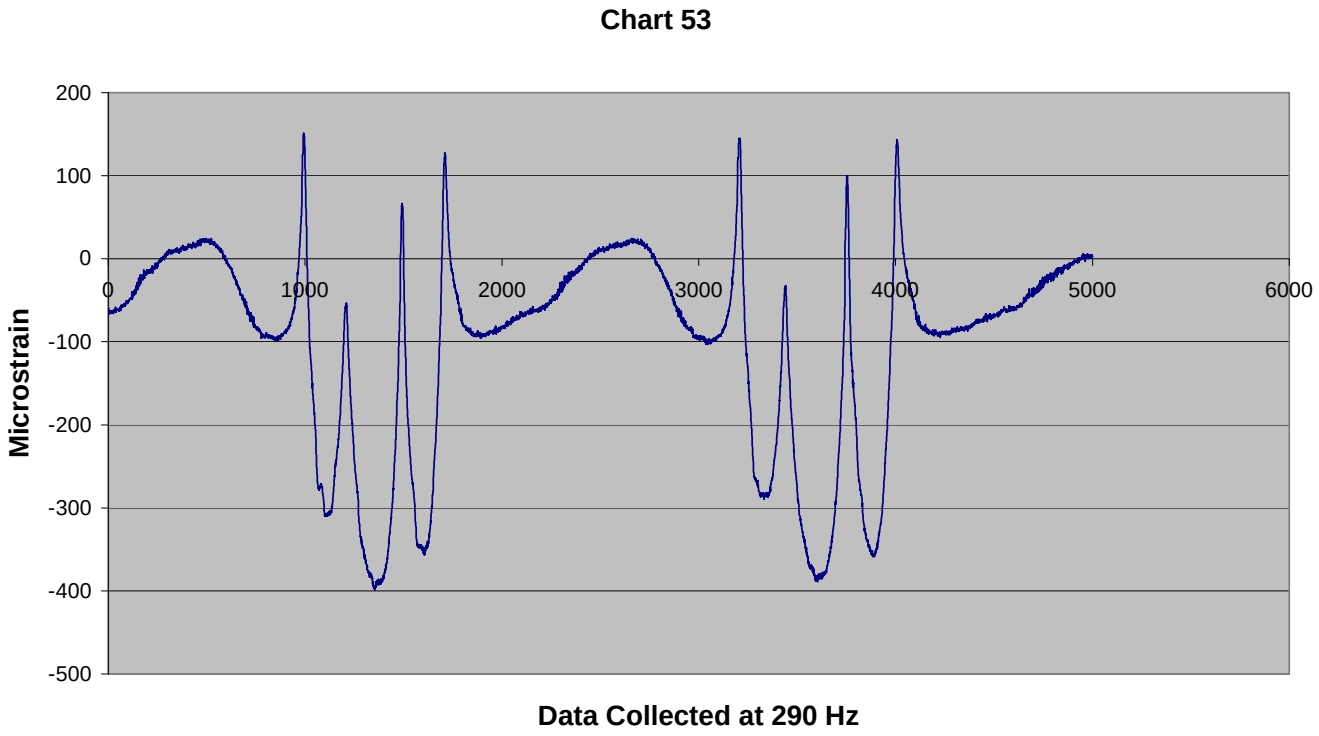


Figure A.2. Strain Data Collected from a Rail with a Train for 7.24 seconds

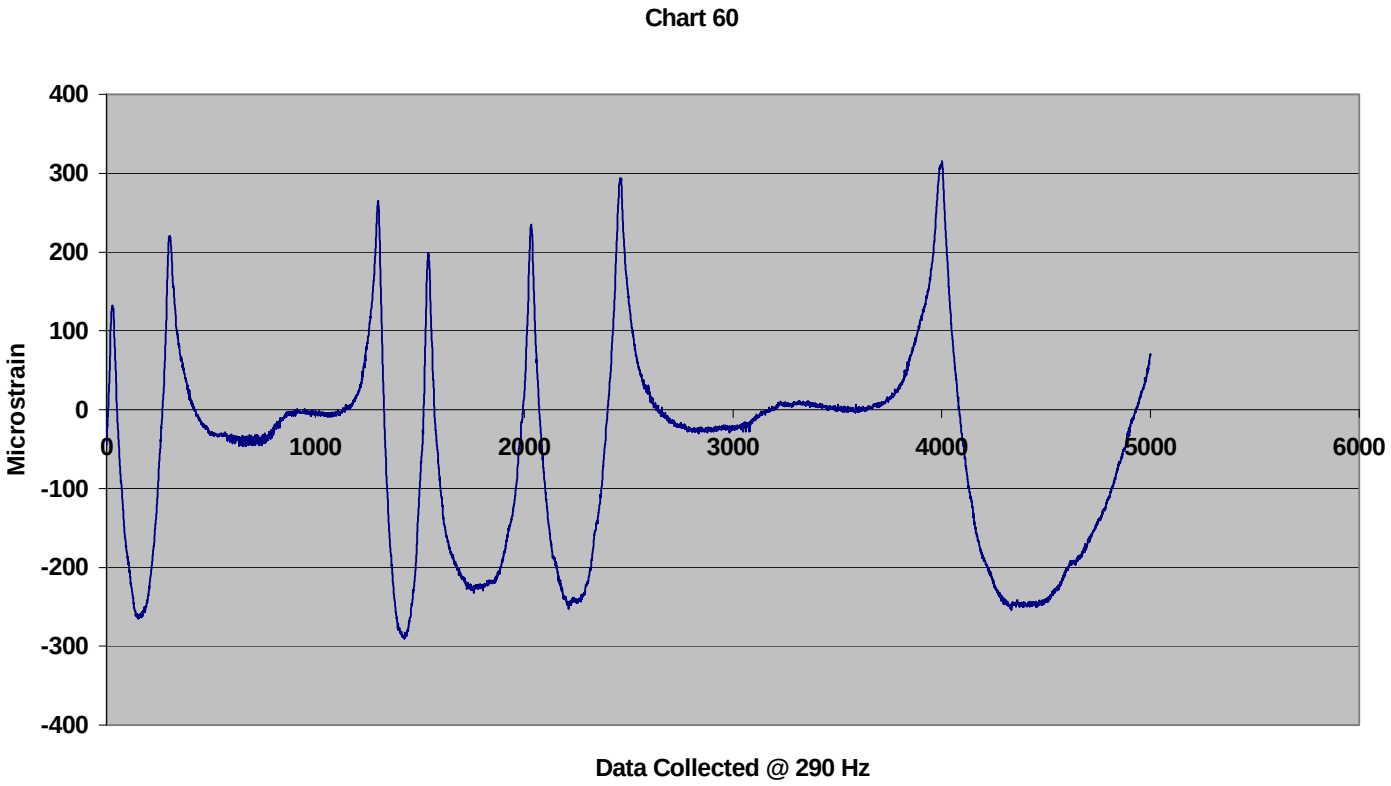


Figure A.3. Strain Data Collected from a Rail with a Train for 7.24 seconds

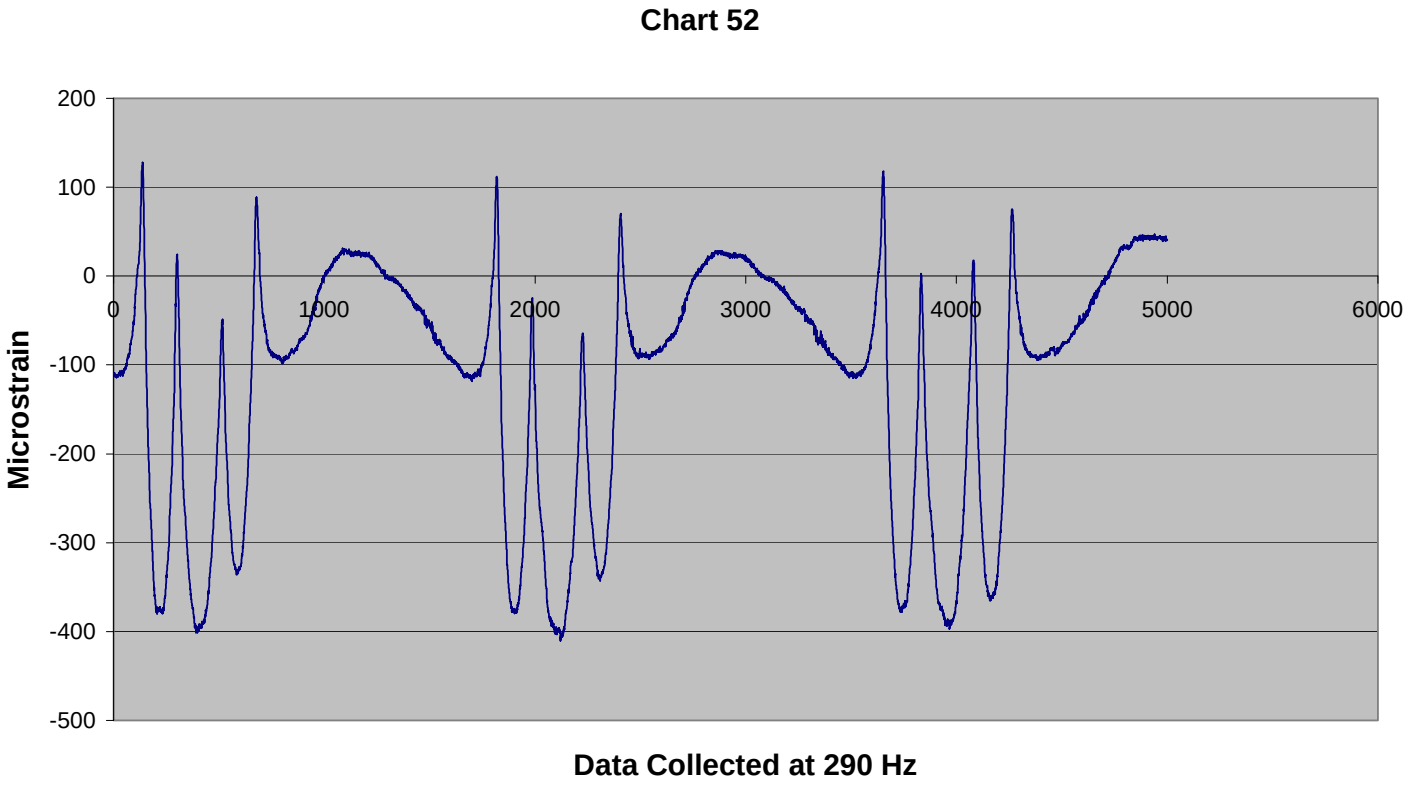


Figure A.4. Strain Data Collected from a Rail with a Train for 7.24 seconds